

Distribution Agreement

In presenting this thesis or dissertation as a partial fulfillment of the requirements for an advanced degree from Emory University, I hereby grant to Emory University and its agents the non-exclusive license to archive, make accessible, and display my thesis or dissertation in whole or in part in all forms of media, now or hereafter known, including display on the world wide web. I understand that I may select some access restrictions as a part of the online submission of tis thesis or dissertation. I retain all ownership rights to the copyright of the thesis or dissertation. I also retain the right to use in future works (such as articles or books) all or part of this thesis or dissertation.

Signature:

Neha Ahuja

Date

Gold(III) Complexes as Potential Anticancer Metallotherapeutics

By

Neha Ahuja
Master of Science

Chemistry

Dr. Cora E. MacBeth
Advisor

Dr. Khalid Salaita
Committee Member

Dr. Emily Weinert
Committee Member

Accepted:

Lisa A. Tedesco, Ph.D.
Dean of James T. Laney School of Graduate Studies

Date

Gold(III) Complexes as Potential Anticancer Metallotherapeutics

By

Neha Ahuja
M.S., University of North Carolina Charlotte, 2010

Advisor: Dr. Cora E. MacBeth

An abstract of
A thesis submitted to the Faculty of the
James T. Laney School of Graduate Studies of Emory University
in partial fulfillment of the requirements for the degree of
Master of Science
In Chemistry
2012

Abstract

Gold(III) Complexes as Potential Anticancer Metallotherapeutics
By Neha Ahuja

Gold(III) complexes are emerging as potential candidates for anticancer metallotherapeutic agents. Gold complexes are proposed to bring about their therapeutic activity in a mechanism different from that of cisplatin.¹ The unique properties of gold are being explored by complexing it with the appropriate ligand scaffold that makes the gold complexes target specific.² This report describes the results for the attempted synthesis and characterization of two Au(III) complexes with the 5-nitro-1,10-phenanthroline and 5-amino-1,10-phenanthroline ligands. The substituted phenanthroline ligands render different properties to their respective complexes in terms of their stability and activity in solution. Previously synthesized 2,9-dialkyl substituted, [(^{sec}-butylphenanthroline)AuCl₃] when tested *in vitro* was found to be more cytotoxic than cisplatin towards selected human cancer cell lines, with their IC₅₀ values 2-8 times lower than the values for cisplatin.³ Substituting functional groups instead of dialkyl groups, on the aromatic backbone lowers the overall hydrocarbon character of the complexes. This would help in enhancing the hydrophilic properties of complexes, which is an essential property required for their *in vitro* cytotoxicity assays, and make them suitable candidates for *in vivo* testing for their applications as anticancer agents. The synthesis and characterization of the Au(III) complexes with the substituted phenanthroline ligands is reported. Cu(II) complexes of the ligands have also been prepared to understand the behavior of gold(III) complexes in solution state and elaborate and compare the chemistry of ligands with other metal centers.

Gold(III) Complexes as Potential Anticancer Metallotherapeutics

By

Neha Ahuja
M.S. Chemistry, University of North Carolina Charlotte, 2010

Advisor: Dr. Cora E. MacBeth

A thesis submitted to the Faculty of the
James T. Laney School of Graduate Studies of Emory University
in partial fulfillment of the requirements for the degree of
Master of Science
In Chemistry
2012

Table of Contents

Section	Page
List of Figures	
List of Schemes	
List of Tables	
List of Equations	
Introduction	1
Au(III) chemistry	1
Ligands and their significance	3
Reducing agents	4
Cisplatin and its mode of action	4
The proposed mitochondrial pathway	5
Results and Discussion	10
Synthesis and spectroscopic characterization of [(^{nitro} phenanthroline)AuCl ₃]	10
Synthesis and spectroscopic characterization of [(^{amino} phenanthroline)AuCl ₃]	16
Stability studies in presence of reducing agents	20
Calculation of logP	26
X-ray Crystallographic studies	27
Alternative synthetic approach	30
Conclusions	40
Experimental	41
References	51

List of Figures

Figures	Page
Figure 1. Auranofin, organogold(III) complex and cisplatin structures	2
Figure 2. Cisplatin mode of action	5
Figure 3. 2,9-dialkyl-phenanthroline and (^{methy} l bipy) Au(III) complexes	7
Figure 4. UV-visible scans for ligand (1) and complex (3) in 0.1 M phosphate buffer	13
Figure 5. UV-visible scans for ligand (1) and complex (3) in 0.1 M phosphate buffer at pH = 7.4, 37 °C at 0 h and 23 h	14
Figure 6. UV-visible spectra showing the red shifting of λ_{max} from the disubstituted bipyridine ligand to its gold(III) complex	15
Figure 7. ¹ H NMR data for complex (3) and ligand (1), overlaid spectra	16
Figure 8. UV-visible scans for ligand (2) and complex (4) in 0.1 M phosphate buffer	18
Figure 9. UV-visible scans for ligand (2) and complex (4) in 0.1 M phosphate buffer at pH = 7.4, 37 °C at 0 h and 23 h	19
Figure 10. GSH studies for ligand (1) and complex (3) at 37 °C	21
Figure 11. Ascorbic acid studies for ligand (1) at 20 °C and complex (3) at 37 °C	23
Figure 12. GSH studies for ligand (2) and complex (4) at 20 °C	24
Figure 13. Ascorbic acid studies for ligand (2) at 20 °C and complex (4) at 37 °C	25
Figure 14. Molecular structure for [^{nitro} phenH] ⁺ [CH ₃ SO ₃] ⁻ , protonated ligand (1)	27
Figure 15. Molecular structure for [^{6-amino,5-chloro} phenH] ⁺ [BF ₄] ⁻ , protonated ligand (2)	28
Figure 16. K _b values for ligand (1) and ligand (2)	30

Figure 17. UV-visible spectra for complex (5) overlaid with spectra for ligand (1), room temperature, (1×10^{-4} M in Methanol); spectra for complex (5) provided as an inset for clarity	34
Figure 18. UV-visible spectra for complex (6) overlaid with spectra for ligand (2), room temperature, (1×10^{-4} M in Methanol); spectra for complex (6) provided as an inset for clarity	35
Figure 19. ESI-MS plots for complex (5), positive and negative mode	36
Figure 20. ESI-MS plots for complex (6), positive and negative mode	37
Figure 21. Targeted structures for complexes (5) and (6)	38

List of Schemes

Schemes	Page
Scheme 1. The proposed mitochondrial TRxR2 pathway	6
Scheme 2. Synthesis of ligand (1) and (2)	10
Scheme 3. Synthesis of complex (3)	11
Scheme 4. Synthesis of complex (3)	11
Scheme 5. Synthesis of complex (3)	12
Scheme 6. Synthesis of complex (4)	17
Scheme 7. Synthetic route for synthesis of complex (3) and (4), from PF_6^- Au(III) salts	31
Scheme 8. Synthesis of complexes (5) and (6)	33

List of Tables

Tables	Page
Table 1. Crystal refinement data for [^{nitro} phenH] ⁺ [CH ₃ SO ₃] ⁻	47
Table 2. Crystal refinement data for [^{6-amino,5-chloro} phenH] ⁺ [BF ₄] ⁻	48

List of Equations

Equations	Page
Equation 1. Reaction equilibrium between the reactants and products in non-aqueous solvents	30

Introduction

Cancer is widely prevalent in today's society and is the leading cause of death amidst the industrial population.⁴ Factors like physical inactivity, aging, smoking and improper diets are considered to play a significant role in the development and progression of cancer.⁴ *Cis*-diamminedichloroplatinum (cisplatin) and some of its analogues are widely administered anticancer drugs. Chemotherapeutic by action, cisplatin primarily targets are the prostate and ovarian cancer cells. Secondary targets of cisplatin include head and neck tumors, small-lung carcinoma and bladder carcinoma.⁵ Although widely used, cisplatin treatment has severe drawbacks associated with its use. DNA is the primary target, and inhibition of DNA replication is the therapeutic mode of action for cisplatin. Shortcomings of the drug arise due to its inability to discriminate between a cancerous cell's and a rapidly dividing normal cell's DNA. Side effects range from severe nausea and vomiting to nephro-, neuro- and ototoxicity. Furthermore, cell lines have either begun to develop resistance or are intrinsically resistant to cisplatin, which affects the drug efficacy when administered.⁵ The side effects associated with cisplatin treatment have resulted in a quest for other non-platinum based drugs with a higher specificity towards the targeted cancer cells and are able to overcome the side effects associated with cisplatin.¹

Au(III) chemistry

Au(III) complexes are emerging as the alternative treatment mode, owing to their antiproliferative and cytotoxic behavior observed both *in vitro* and *in vivo*.¹ Archeological records trace the history of gold and its medicinal properties in several cultures.

Treatment with gold-based drug is also known as chrysotherapy and is a well-established mode of treatment used for rheumatoid arthritis (RA).^{1,6} Inspiration for using gold complexes as potential anticancer metallotherapeutics stems from the discovery of a decreased extent of cancer susceptibility in patients treated with gold drugs for RA.⁷ Au(I) complexes (e.g. auranofin) are the widely administered drugs for the treatment of RA (Figure 1).⁶ Studies into the mechanistic activities of auranofin led to the observation of the cytotoxicity of auranofin against tumor cells *in vitro*.²

Due to this, several Au(I) phosphine complexes were prepared and tested for their antitumor activity. Meanwhile Au(III) complexes were being investigated for their activity *in vitro* as the Au(III) is isoelectronic to Pt(II), in having a d^8 electron count in its outermost shell. Based on this, it was hypothesized that Au(III) could bring about the therapeutic action of cisplatin.^{2,8} However, the initially prepared Au(III) complexes were found to be thermodynamically unstable and light sensitive, undergoing reduction to Au(I) or Au(0) in presence of reducing agents. Owing to this, the quest for gold drugs was abandoned.¹

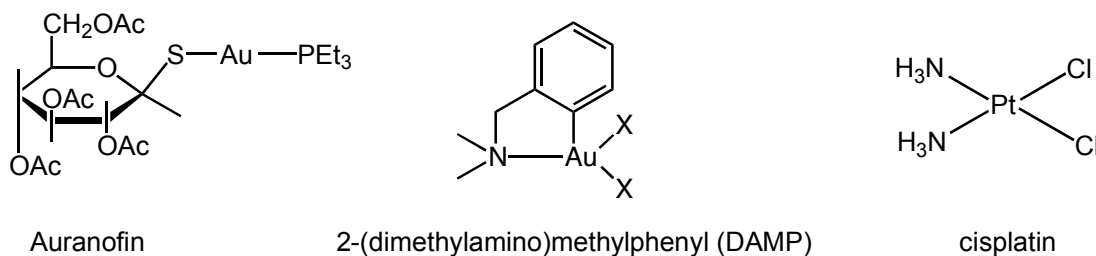


Figure 1. Auranofin, organogold(III) complex and cisplatin structures

Revival of Au(III) chemistry occurred in the 1990's with the synthesis of organogold(III) complexes (e.g. Au(III)DAMP) and several other complexes that were square-planar cisplatin analogues with a higher stability profile and encouraging *in vitro* cytotoxicity(Figure 1.).¹

Ligands and their significance

The choice of ligands is critical in synthesis of metal-based pharmaceutical complexes. With an appropriate choice of ligands the overall charge on the system can be modulated and a balance of the hydrophilic and lipophilic properties of a complex can be established.⁶ Studies conducted demonstrated how the nature of ligand bound to the metal center was playing a critical role.² The Au(III) center which is kinetically labile was found to be stabilized by bi, tri or multidentate ligand scaffolds with N or O donor atoms.⁶ Researchers have utilized polydentate ligands like polyamines, cyclam, terpyridines, porphyrins and phenanthrolines, aromatic systems with nitrogen donor atoms, for researching the anti-proliferative mechanism of Au(III) complexes and understanding the therapeutic pathways adopted by these agents to destroy the cancer cells.^{9-9b} These ligands have been shown to strongly stabilize the Au(III) center by decreasing its overall reduction potential. The chelate effect may also act as the driving force for discouraging unfavorable reactions.² Moreover, the presence of nitrogen donor ligands have been shown to prevent ligand exchange from occurring in solution state, a commonly observed feature leading to reduction of Au(III) in biological solutions.⁶

Reducing agents

Reducing agents like glutathione (GSH) and Ascorbic acid (Aa) are commonly found within the intracellular environment. GSH plays a vital role in maintaining the intracellular redox balance and controls the generation of Reactive Oxygen Species (ROS) such as H_2O_2 thereby detoxifying the cell.¹⁰ The GSH is a non-protein thiol, and is present in its reduced state within the cells. The oxidation cycle of GSH to GSSG during H_2O_2 reduction cycle involves a Se-dependent pathway.¹¹ This route involves the formation of a selenol group (R-SeH), this selenol group has a high affinity for Au and can bring about a reduction of the Au(III) center. Presence of chelate ligands with N donor atoms, that have a higher affinity for the Au(III) cation and do not undergo displacement easily thereby preventing the reduction of Au(III).^{6, 10}

Cisplatin and its mode of action

Cisplatin's chemotherapeutic activity is due to formation of platinum-DNA adducts. The proposed mechanism of action in case of cisplatin and other platinum based drugs is inhibition of cell growth by cross-linking of cisplatin with DNA (Figure 2.) and opening up the helix to a point where it cannot be annealed back. The DNA cross-links formed by cisplatin may be inter- or intrastrand with a high specificity towards the N7 of guanine base of DNA, as it is extremely nucleophilic.¹² This brings about a disruption of the cell growth, and this process hinders DNA repair mechanisms. This leads to trigger of a series of intracellular events, ultimately causing apoptosis (cell death), and DNA is digested by the endonuclease enzymes.^{5, 12} Research with the Au(III) complexes have so far demonstrated to bring about a mitochondrial damage of the cells by interacting with

specific proteins instead of producing lesions in the DNA, a mechanism unlike that of cisplatin.^{9a}

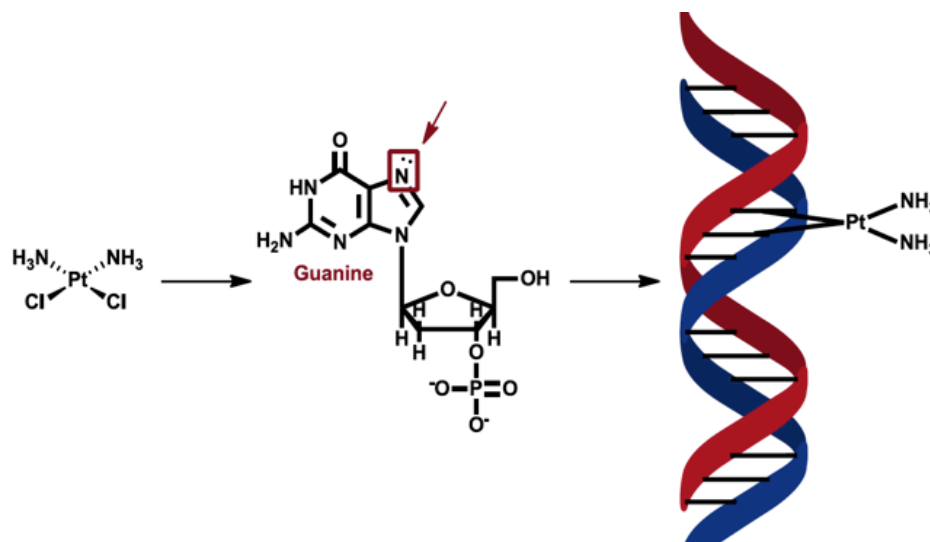


Figure 2. cisplatin mode of action^{3, 13a-b}

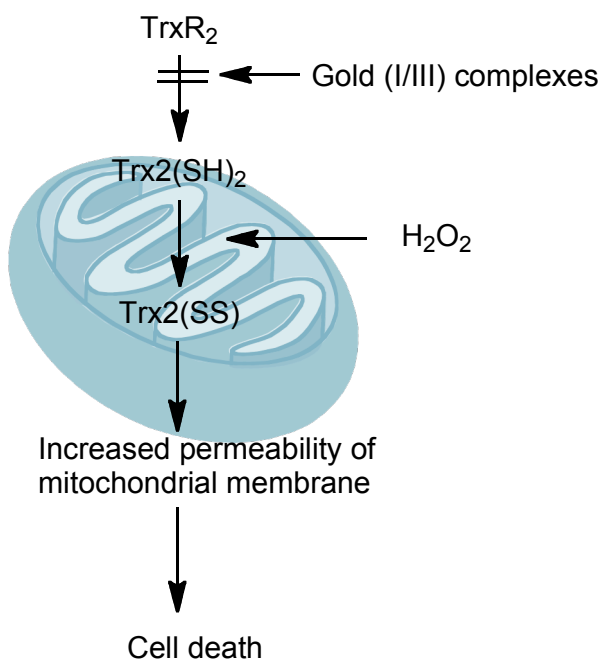
The proposed mitochondrial pathway

Most of the mechanistic studies carried out for gold complexes indicate mitochondria is the target. Mitochondria is the powerhouse of a cell and also contains the enzyme thioredoxin reductase (TrxR2), which is found to be up regulated in the case of cancer cells.² When tested, several of the Au(III) compounds have demonstrated an efficient inhibition of this mitochondrial enzyme.¹⁰

Mammalian Thioredoxin (Trx2), found in the mitochondria, is a homodimeric flavoprotein that contains a redox active site. The reduction of oxidized Trx2 is catalyzed by TrxR2, which involves the reduction of disulfide to a dithiol. This dithiol form is an important cellular reductant involved in DNA synthesis, and in defense system against

oxidative stress. The C-terminus of TrxR2 contains a 16-residue extension with a Gly-Cys-SeCys-Gly sequence that is found conserved in all mammalian TrxR. The TrxR is one of the selenoenzyme's involved in the detoxification process.¹⁰ In TrxR, the selenocysteine residue (SeCys) is essential for the catalytic activity of TrxR2. If the selenium is removed or alkylated the TrxR2 becomes inactive.¹⁴

Trx2 is oxidized by H_2O_2 released as a by-product of mitochondrial respiration. The Au(III) complexes are proposed to selectively modify the selenol active site by binding to it.¹⁵ On binding of Au(III) to the selenocysteine group the TrxR2 is rendered inactive, thereby inhibiting the reduction of the oxidized Trx2 by TrxR2. The built up peroxide and oxidized Trx2 target the intramitochondrial processes and bring about the formation of a transition pore, increasing the permeability of the mitochondrial membrane (Scheme 1).^{2, 10}



Scheme 1. The proposed mitochondrial TRxR2 pathway^{2, 10}

When compared to the normal cells the cancerous cells have a decreased extent of transition through the mitochondria.¹⁰ This increase of membrane permeability results in the trigger of apoptosis, thus bringing about the therapeutic action of gold complexes.^{2, 10} Alternative mode of action adopted by Au(III) drugs is possibly the reason for their activity against some of the cisplatin resistant cell lines.^{2-3, 10, 14}

Au(III) complexes with phenanthrolines as ligands hold promising outcomes as anticancer metallotherapeutics.³ The phenanthroline (phen) ligand is bidentate with nitrogen donor atoms that can potentially protect the gold center from undergoing rapid reduction in a biological milieu. Along with this, phenanthroline complexes with other metals like palladium, lanthanum and rhodium have also demonstrated anticancer activity when tested *in vitro*.^{16a-c} However, very few Au(III) complexes with phenanthroline ring system have been synthesized and reported.^{3, 8} In the past, our research laboratory has explored the coordination chemistry of substituted phenanthroline ligands and prepared gold complexes with the 2,9-dialkylphen ligands [(^Rphen)AuCl₃] (R = *n*-butyl, *sec*-butyl).⁸ Presence of the substituent groups (Figure 3.) sterically protects the Au(III) from reduction in presence of intracellular reducing agents like glutathione and ascorbic acid.

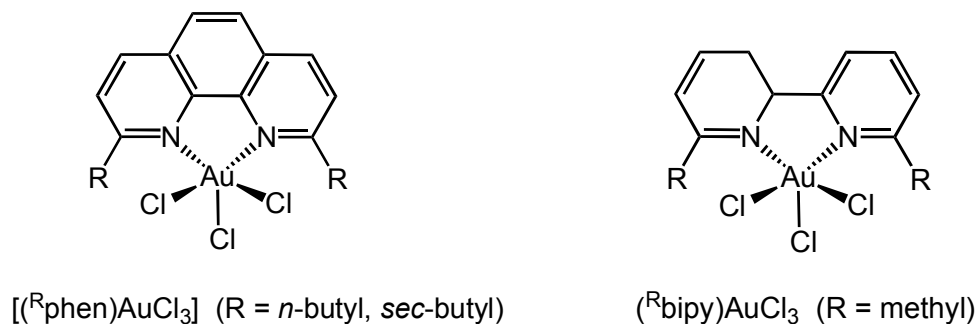


Figure 3. 2,9-dialkyl-phenanthroline and (^{methyl}bipy) Au(III) complexes

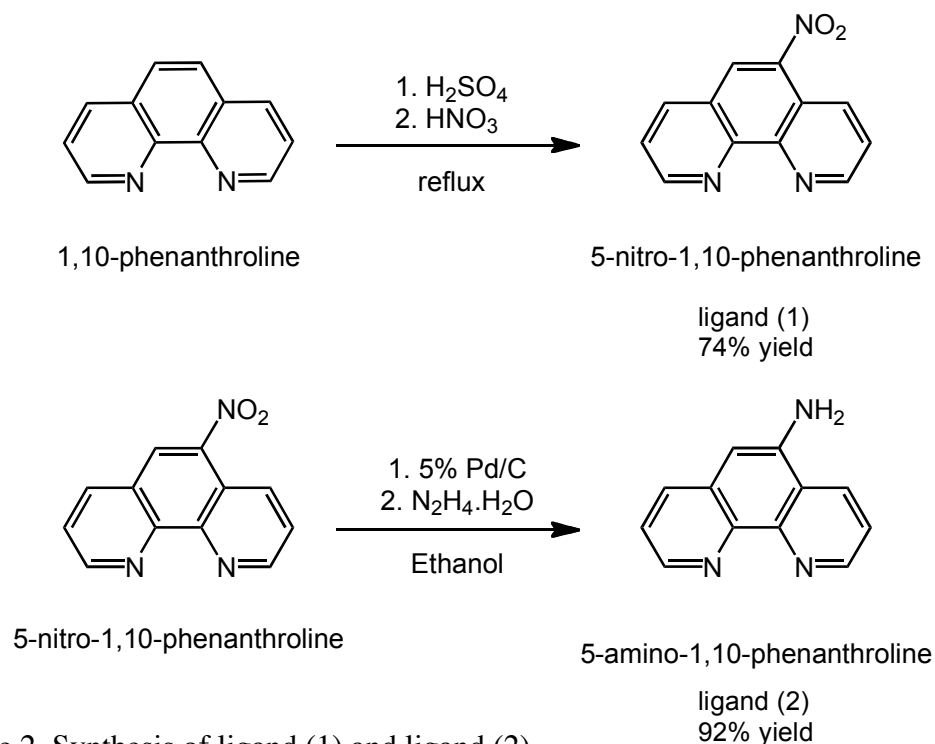
The presence of alkyl substituents was predicted to hinder DNA binding activity along with providing steric protection to Au(III).¹⁷ The dialkyl phen complexes were successfully synthesized and the chemistry was extended to prepare Au(III) complexes with 6,6'-disubstituted bipyridine (^Rbipy) as ligand, with the [(^{methyl}bipy)AuCl₃] complex (Figure 3.) being successfully prepared and characterized.³ Additionally the *in vitro* cytotoxicity, DNA binding and the stability profiles in buffered solutions in presence of reducing agents for the [(^{methyl}bipy)AuCl₃] and the dialkyl phen complexes were also determined.³ An *in vitro* study with the dialkyl phen ligands and their complexes and with [(^{methyl}bipy)AuCl₃] against selected head, neck, lung cancer cell lines displayed that [(^{sec-butyl}phen)AuCl₃] displayed a higher level of cytotoxicity when compared to cisplatin. The half minimum inhibitory concentration (IC₅₀) values for [(^{sec-butyl}phen)AuCl₃] complex were found to be 2-8 times lower than the values for cisplatin. The presence of bulky alkyl substituents were found to sterically protect the Au(III) center from getting easily reduced in solution that may have contributed to an enhancement of their cytotoxic potential. These promising results motivated us to further expand the phenanthroline ligand family to prepare ligands that could provide the same level to an enhanced extent of stability in solution and cytotoxicity when tested *in vitro*.³

For this study, the phen ligand chemistry has been extended to study the effects of changes in the electronic environment of the aromatic ligands on the synthesis of complexes, their solution stability, cytotoxic profiles and DNA binding. Substitutions with an electronegative group (NO₂) and with an electron-donating group (NH₂) on the aromatic backbone generated ligand scaffolds with different electronic environments.

Presence of the substituents on the aromatic backbone provides us with a ligand scaffold with a lower extent of hydrocarbon character and renders different basicity profiles to the nitrogen donor atoms of the phenanthroline ring system. We hypothesize that these individual properties of the ligands will be manifested in the nature and reactivity pattern of the Au(III) complexes prepared with the respective ligand scaffolds. The work that has been conducted and described herein will provide an extended picture to compare and understand the changes in Au(III) complex activity based on the type of ligand coordinated. This study aims at preparing the novel Au(III) complexes and evaluating the solution stability and cytotoxic potentials of the complexes prepared and further explore the structure activity relationship.

Results and Discussion

Synthesis of ligands 5-nitro-1,10-phenanthroline, ligand (1) and 5-amino-1,10-phenanthroline, ligand (2) was successfully carried out using the literature procedure.¹⁸ The ligands were observed as pure crystalline solids in good yields (Scheme 2.) and were preliminarily characterized by NMR, IR and UV-vis spectroscopies.

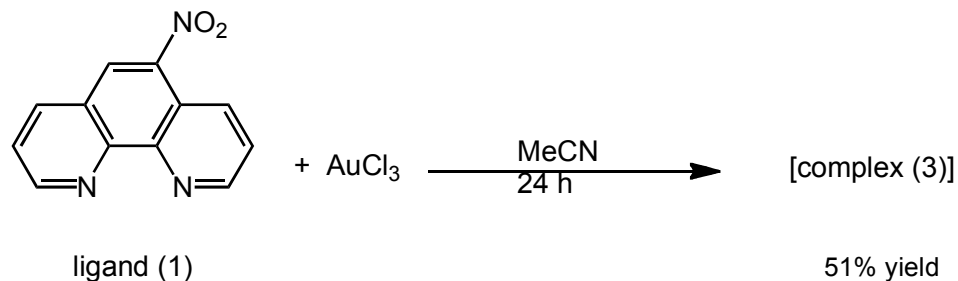


Scheme 2. Synthesis of ligand (1) and ligand (2)

Synthesis and spectroscopic characterization of [(^{nitro}phenanthroline)AuCl₃]

The synthesis of dialkyl phenanthroline gold complexes utilized the sodium tetrachloroaurate dihydrate (NaAuCl₄•2H₂O) with the (^Rphen) and the (^{methyl}bipy) ligands in presence of Ag(I) salts that afforded the corresponding dialkyl phenanthroline Au(III) complex. Interested in exploring alternative routes, a direct approach of using Au(III)chloride as the reagent for metallation was attempted. Reaction of the ligand (1)

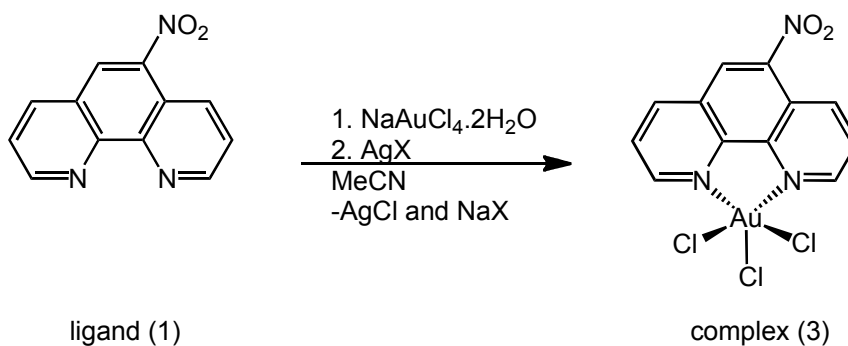
with AuCl_3 in a 1:1 stoichiometric ratio, as per (Scheme 3.) to prepare the $[(\text{nitrophenanthroline})\text{AuCl}_3]$, complex (3).



Scheme 3. Synthesis of complex (3)

This protocol resulted in the formation of the product, complex (3) along with unreacted ligand (1) with their percent yields in a 45:50 ratio. The ^1H NMR of the complex (3) in DMSO-d_6 showed that the reaction had not reached completion. The reaction was observed to reach completion after sample was allowed to stand in DMSO-d_6 for two days before taking a ^1H NMR spectrum.

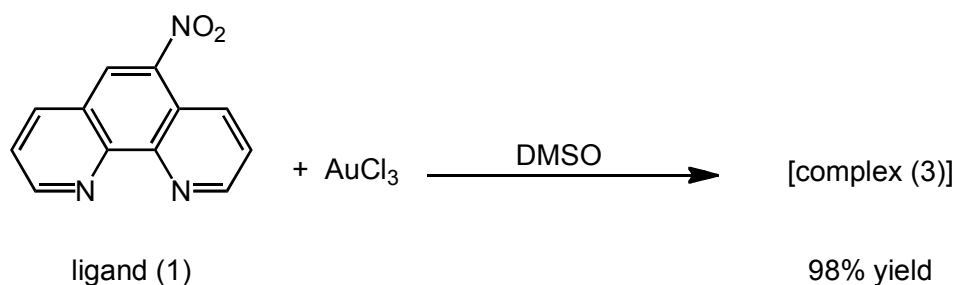
Following this observation a different approach for metallation was used for product synthesis. As carried out for the R^{phen} and the $\text{methyl}^{\text{bipy}}$ ligands the $\text{NaAuCl}_4 \cdot 2\text{H}_2\text{O}$ and Ag(I) salt were used as a halide abstracting agent (Scheme 4.).



Scheme 4. Synthesis of complex (3)

Although successful in synthesis of complex (3), the ^1H NMR spectrum of the product still displayed peaks in addition to the complex peaks, indicating the reaction had not reached completion.

Since the reaction was observed to reach completion when allowed to stand in DMSO-d_6 , the complex synthesis was reattempted with DMSO as the solvent (Scheme 5.). The product isolated when characterized by ^1H NMR displayed the chemical shifts for the aromatic protons of complex (3) and the ligand peaks were absent indicating that the reaction had reached completion.



Scheme 5. Synthesis of complex (3)

The UV-vis spectrum for complex (3), at a concentration of 1×10^{-5} M, in a phosphate buffered solution at $\text{pH} = 7.4$ over a time period of 24 hours shows that the complex (3) is stable in the solution state. The spectrum also displays a small shift in the absorption maxima for the intraligand absorption bands centered 242 and 280 nm, when compared to the UV-vis spectrum of the free ligand with intraligand charge transfer bands centered at 239 and 274 nm and a shoulder peak at 324 nm. The complex (3) shows a weak broad shoulder band from 314-334 nm (Figure 4.). In general the LMCT band generally occurs from 300-400nm and is a characteristic band for the Au(III) chromophore.¹⁹ The

spectrum shows a weak shoulder in the LMCT region versus a stronger absorption profile, as expected upon metallation. The IR spectrum for the ligand (1) displays the NO_2 stretching frequencies, $\nu(\text{NO}_2 \text{ asymmetric})$ at 1518 cm^{-1} and $\nu(\text{NO}_2 \text{ symmetric})$ at 1346 cm^{-1} and for the complex (3) $\nu(\text{NO}_2 \text{ asymmetric})$ at 1524 cm^{-1} and $\nu(\text{NO}_2 \text{ symmetric})$ at 1351 cm^{-1} . The small changes in the UV-visible spectrum and IR stretching frequencies do not completely support successful complex formation.

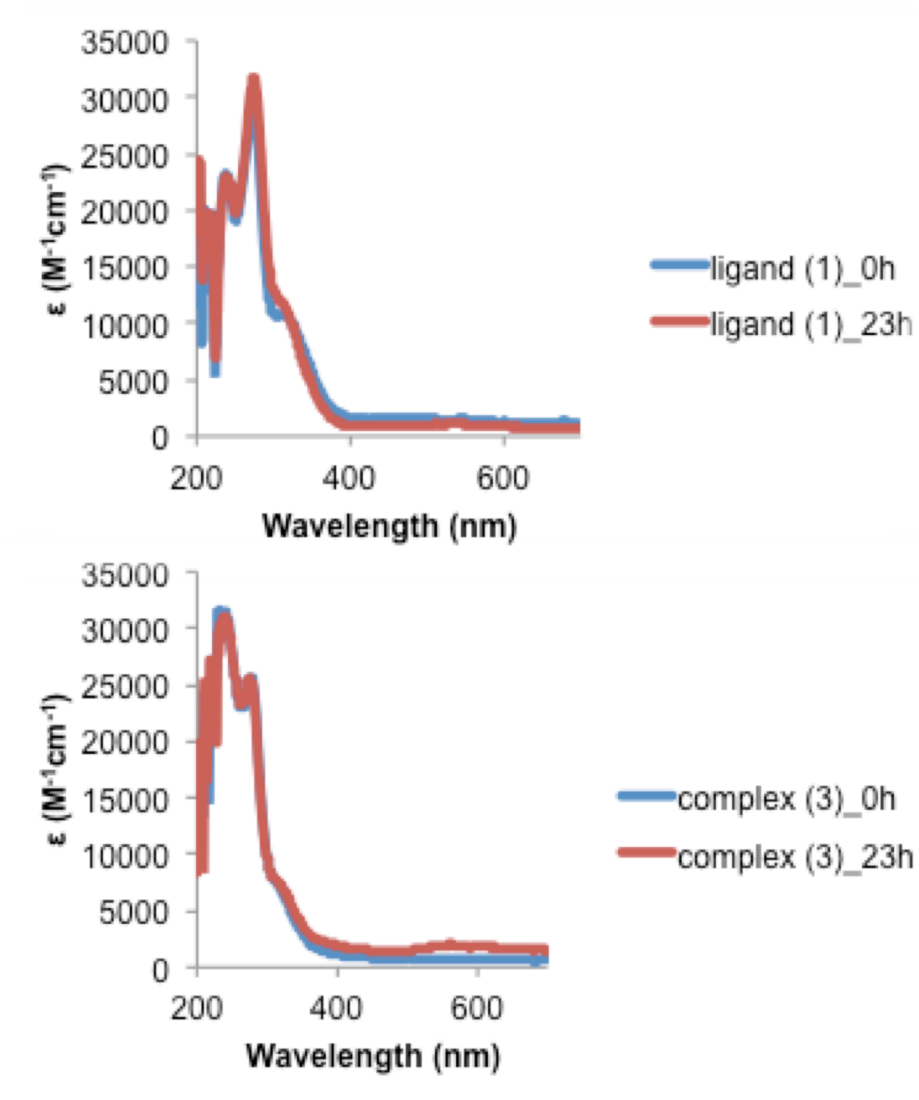


Figure 4. UV-visible scans for ligand (1) and complex (3) in 0.1 M phosphate buffer

A comparison of the UV-Visible spectra for ligand (1) and complex (3) in phosphate buffer under physiological conditions (Figure 5.) does not display a significant red shift of the λ_{\max} as expected, and has been previously observed for other gold(III) complexes prepared with substituted phenanthroline and bipyridine ligands (Figure 6.).^{3,8,17}

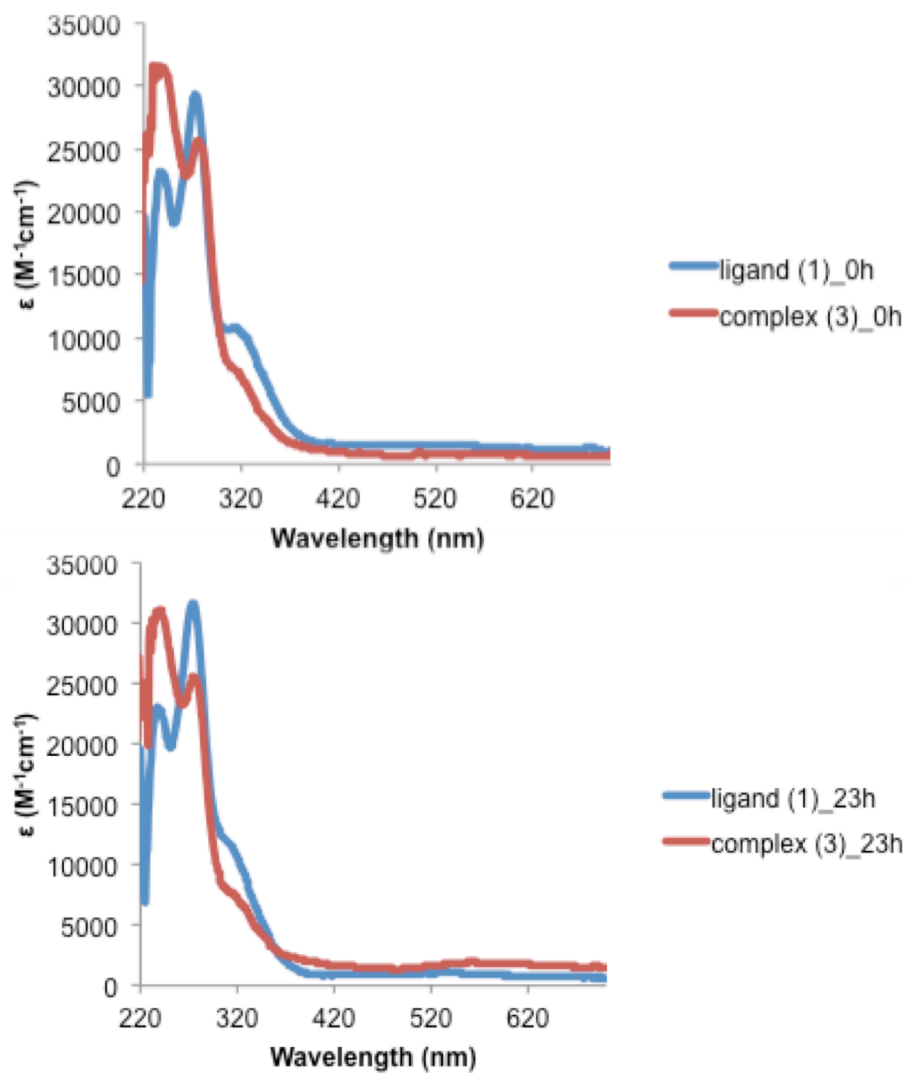


Figure 5. UV-visible spectra for ligand (1) and complex (3) in 0.1 M phosphate buffer at pH = 7.4, 37 °C at 0 h and 23 h

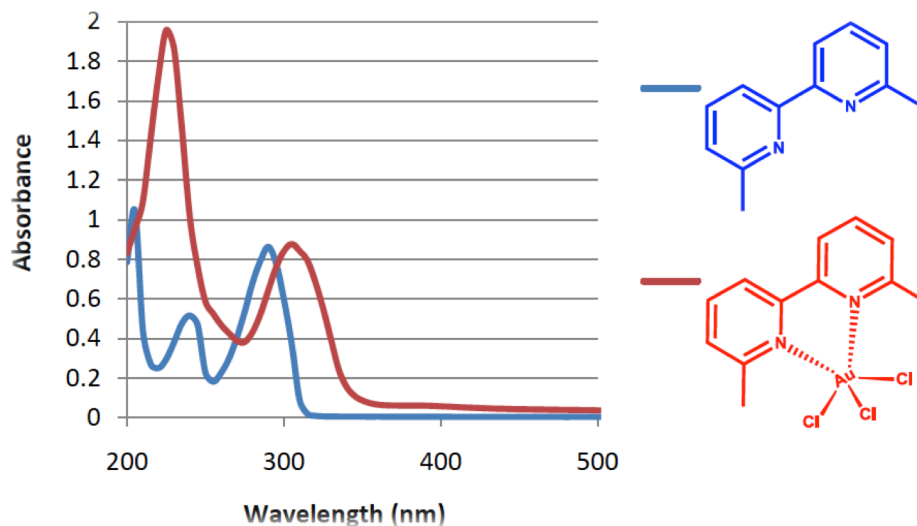


Figure 6. UV-visible spectra showing the red shifting of λ_{\max} from the disubstituted bipyridine ligand to its gold(III) complex

These initial spectroscopic data are suggesting the presence of a cationic species, instead of a neutral complex (3) in the solution state. The ^1H NMR data for ligand (1) when compared to the NMR data for complex (3), does not display a significant downfield shift for the aromatic phenanthroline protons (Figure 7.) as expected for a ligand upon metallation. The data for complex (3) also shows a peak at 4.30 ppm that corresponds to the ^1H resonance from N-H hydrogen. The prepared complex (3) was also found to be insoluble in organic solvents such as chloroform, dichloromethane, acetonitrile and was found to be soluble only in DMSO and DMF, suggesting the presence of a charged species instead of a neutral complex. These results supported the presence of a protonated ligand versus a neutral gold(III) complex with ligand (1).

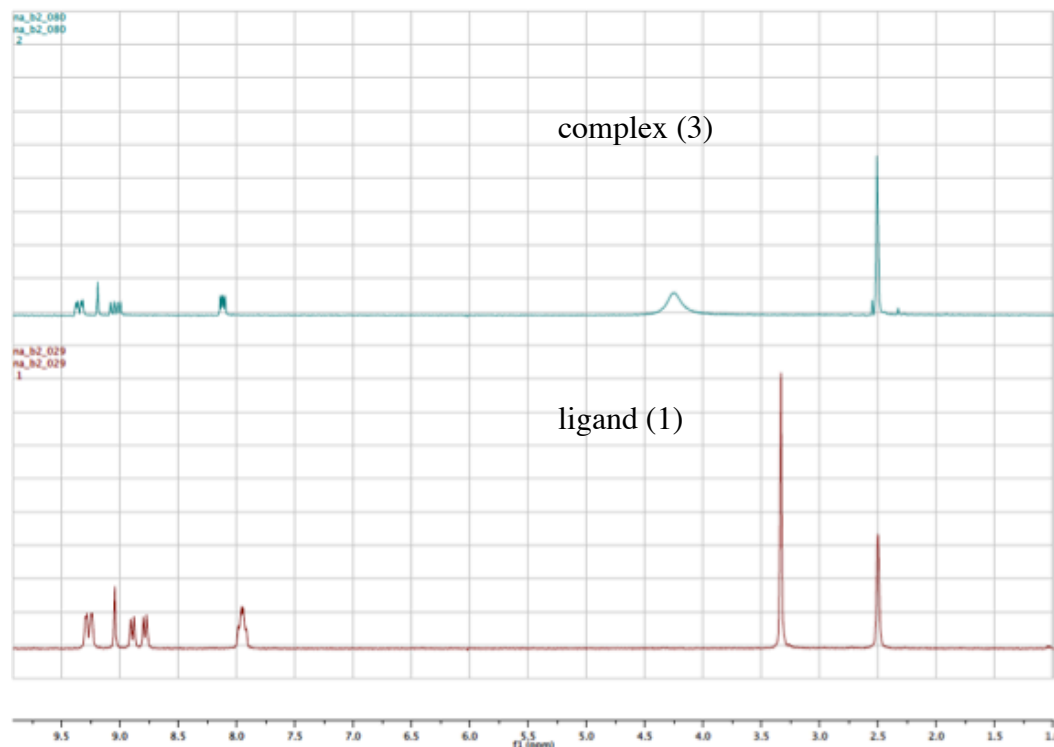
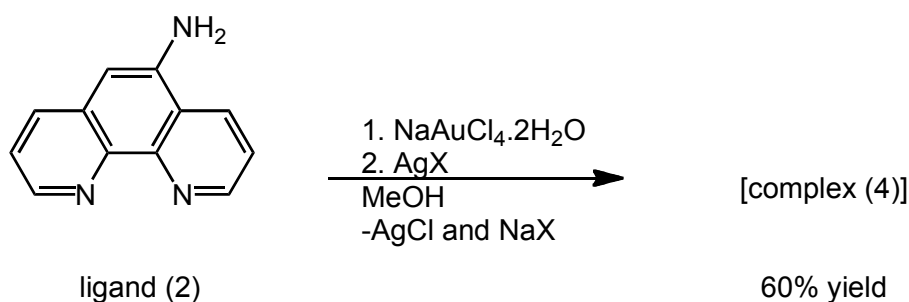


Figure 7. ^1H NMR data for complex (3) and ligand (1), overlaid spectra

Synthesis and spectroscopic characterization of [(^{amino}phenanthroline) AuCl_3]

The synthesis of complex (4) was attempted by refluxing the ligand (2) with AuCl_3 in a one to one stoichiometric ratio with acetonitrile as the solvent. The product was found to be a mixture of ligand (2) and complex (4), as observed by ^1H NMR. Owing to this, another approach towards the synthesis of complex (4) was adopted. The ligand (2) was refluxed with the reagents $\text{NaAuCl}_4 \cdot 2\text{H}_2\text{O}$ and AgBF_4 in methanol for a period of 24 h (Scheme 6.). Methanol was chosen as the solvent as the ligand and the reagents were completely soluble in it. The isolated product was characterized by NMR, IR spectroscopies and ESI-MS techniques.



Scheme 6. Synthesis of complex (4)

The ^1H NMR spectrum for the complex in DMSO-d_6 displays a downfield shift of 0.19 - 1.02 ppm for the amine and the aromatic protons with respect to the spectrum of the ligand (2). The protons of the amine substituent show a broadened signal. This broadening of peaks may be attributed to the rapid proton exchange occurring in the product solution during the NMR experiment or due to H-bonding.

The UV-visible absorption spectra for the complex (4) and the ligand (2) were carried out in a phosphate buffered solution at pH 7.4 at 20 °C and demonstrate stability of the ligand (2) and the complex (4) in solution state. The λ_{max} for the intraligand absorption for the complex (4) are centered at 227, 267 and 290 nm, with the LMCT band as a broad shoulder ranging from 355-372 nm. The absorption maxima for the complex (4) are different from that of the ligand (2), but a significant red shift of the λ_{max} is not observed for complex (4) thereby suggesting absence of a neutral complex (4) in solution (Figure 8.).

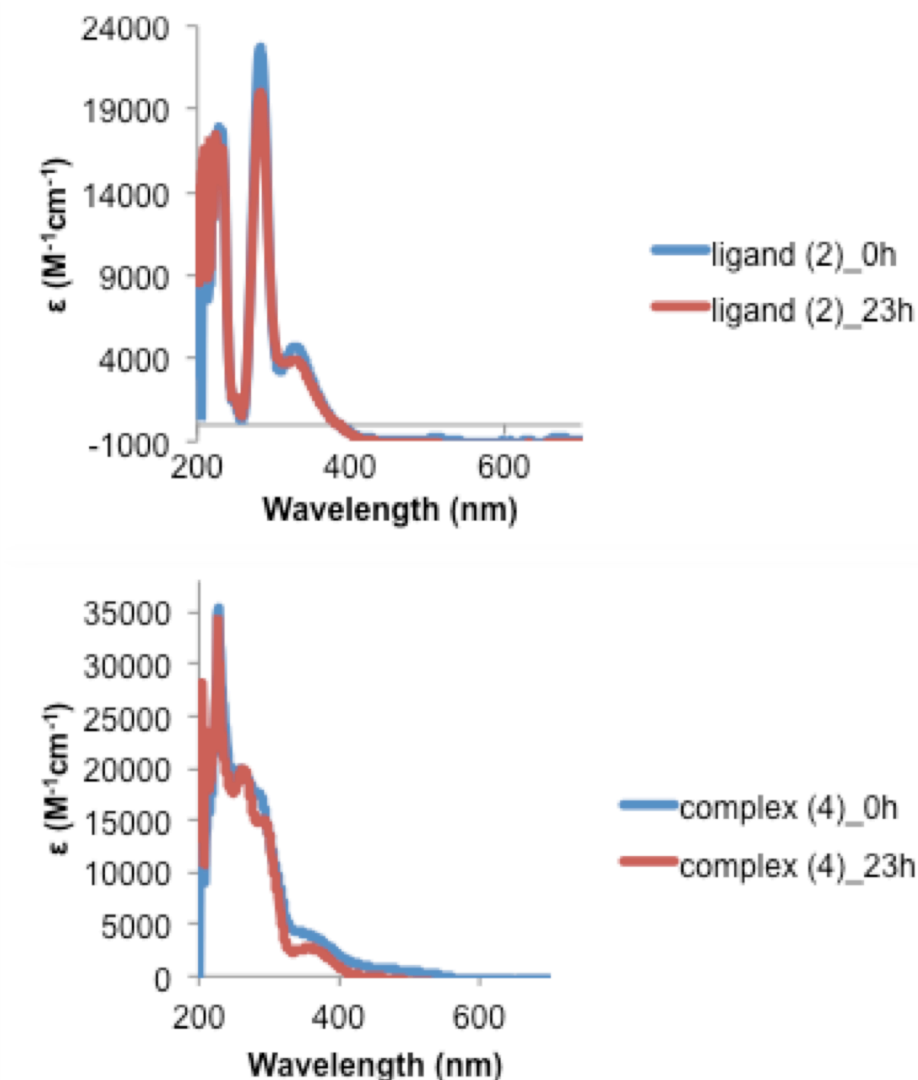


Figure 8. UV-visible scans for ligand (2) and complex (4) in 0.1 M phosphate buffer

A comparison of the UV-visible spectra for ligand (2) and complex (4) shows no significant shifting of the λ_{max} in solution (Figure 9.), from ligand (2) to that of complex (4). Solubility tests conducted on both the compounds demonstrated insolubility of complex (4) in organic solvents, poor solubility in alcohols and high solubility in DMF and DMSO. The ligand (2) was found to be soluble in several organic and polar solvents.

These results suggested the presence of a cationic ligand species instead of a neutral complex (4) in the solution state.

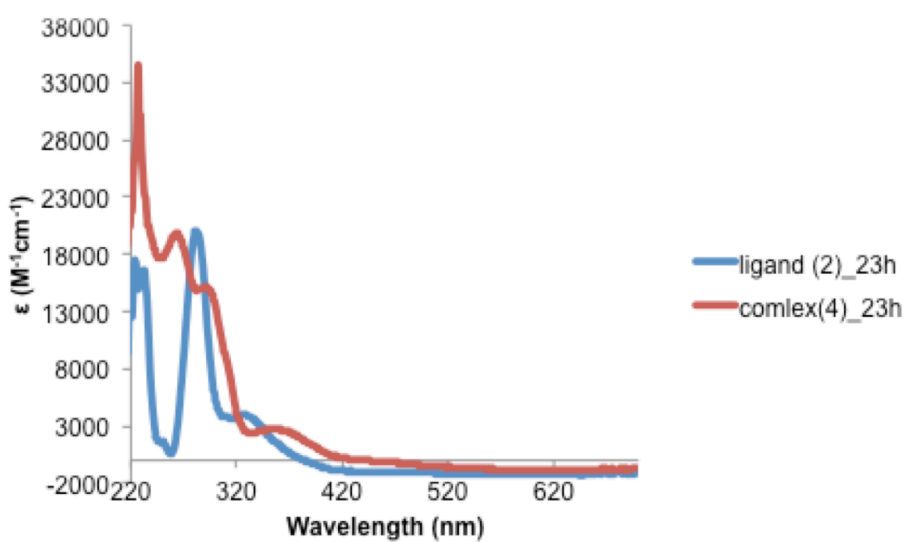
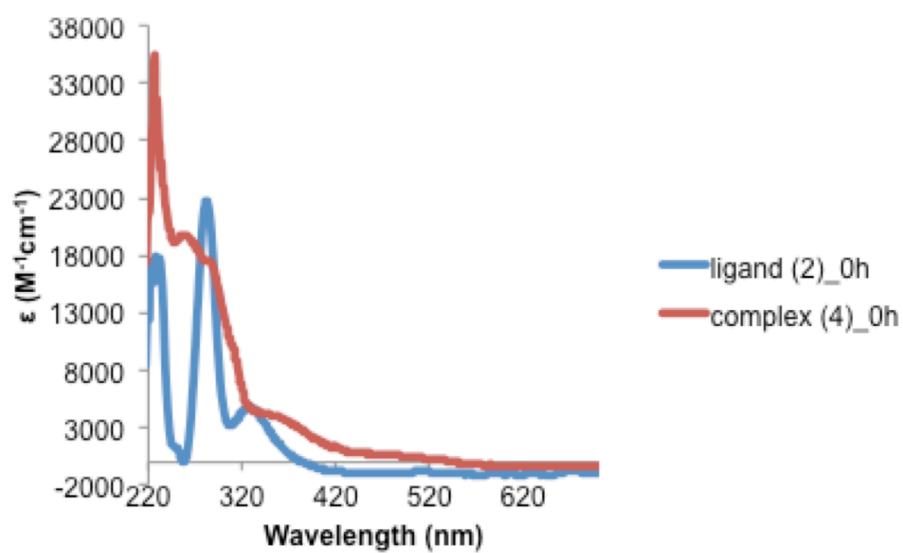


Figure 9. UV-visible spectra for ligand (2) and complex (4) in 0.1 M phosphate buffer at pH = 7.4, 37 °C at 0 h and 23 h

Based on the results and observations so far, further studies are being conducted to acquire data to corroborate the presence of a charged species, instead of a neutral complex (3) and (4) in the solution state.

Stability studies in presence of reducing agents

The stability of the ligands (1 and 2) and the complexes (3 and 4) was carried out in physiological buffered solution. The stability profile for the compounds has also been studied in presence of reducing agents like glutathione (GSH) and ascorbic acid (Aa) over a time period of 24 hours at 20 °C and at 37 °C for complex (3) and complex (4). The ligand and the complex solutions were prepared in DMSO. The studies were carried out at 1×10^{-5} M of complex and GSH, in phosphate buffer at pH = 7.4.

The stability profiles of complex (3) and the ligand (1) in presence of GSH do not display any significant changes in their UV-visible spectrum over 24 hours. The spectra observed are quite similar to those observed for the stability profile studies without the reducing agents. At 20 °C, the λ_{max} for the ligand (1) does not decrease with increasing time, and the absorption profile for complex (3) displays a negligible decrease for the LMCT band (Figure 10.).

This data demonstrates that the Au(III) center is being retained in the solution, since the LMCT band, a characteristic of the Au(III) chromophore, is not completely lost.²⁰ Formation of gold(I) characterized by a band at 450-520 nm in the UV-vis is not

observed in the spectrum. The GSH studies for complex (3) at a higher temperature (i.e. 37 °C) were also carried out.

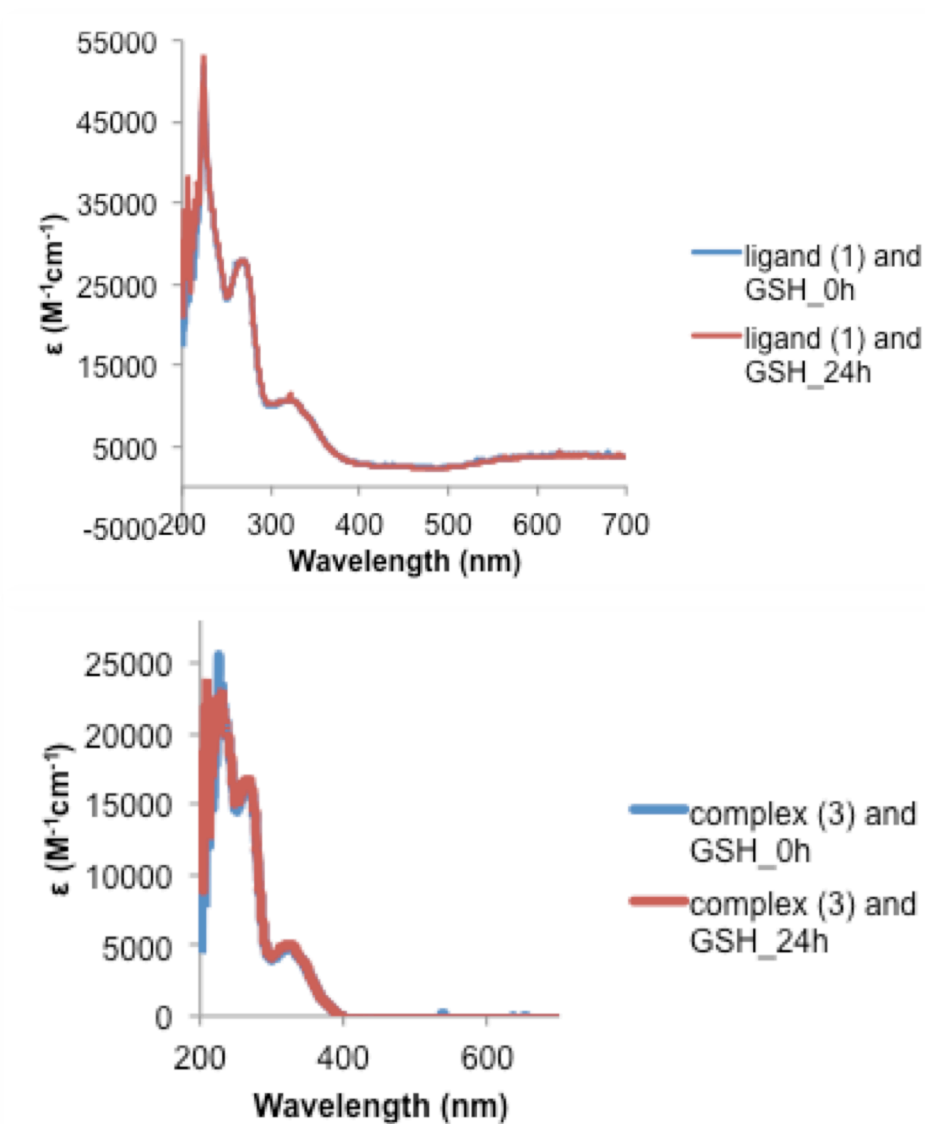


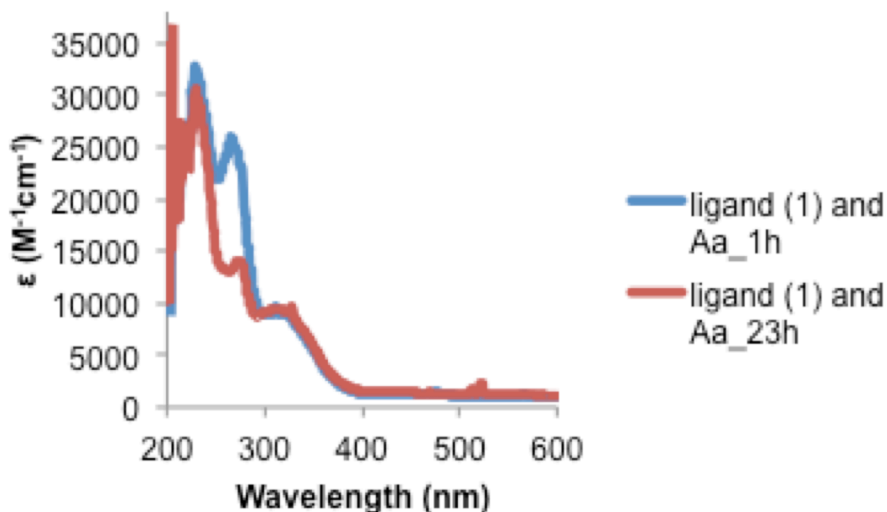
Figure 10. GSH studies for ligand (1) and complex (3) at 20 °C

The stability profiles for ligand (1) and complex (3) were also evaluated in presence of ascorbic acid, another common biological reducing agent. The ligand (1) and the complex

(3) solutions were prepared in DMSO and the studies were carried out in phosphate buffer at pH = 7.4. The data for the complex (3) was acquired at 20 °C and at 37 °C.

The ligand (1) in presence of ascorbic acid at 20 °C, displays a progressive decrease in its intraligand absorption bands for the first 5 hours, after which the decrease in the intensity of the bands is quite less (Figure 11.). This decrease in the intensity of intraligand absorptions bands can be attributed to a reduction of the nitro substituent on the ohenanthroline ring in ligand (1), in presence of a mild reducing agent, ascorbic acid.²¹ Complex (3), in the presence of the reducing agent shows a progressive decrease in its intraligand charge transfer band intensities. The LMCT band (315-330 nm) for complex (3) does not display any significant changes.

The absorption spectrum for complex (3) in presence of ascorbic acid at 37 °C shows a slightly different behavior (Figure 11.).



The intraligand absorption band centered at 230 nm increases in intensity, while the absorption band at 279 nm and the LMCT band display progressive decreases in their

intensity (Figure 11.). An increase of temperature is probably promoting faster aquation rates for the complex with the Au center in its +3 oxidation state.

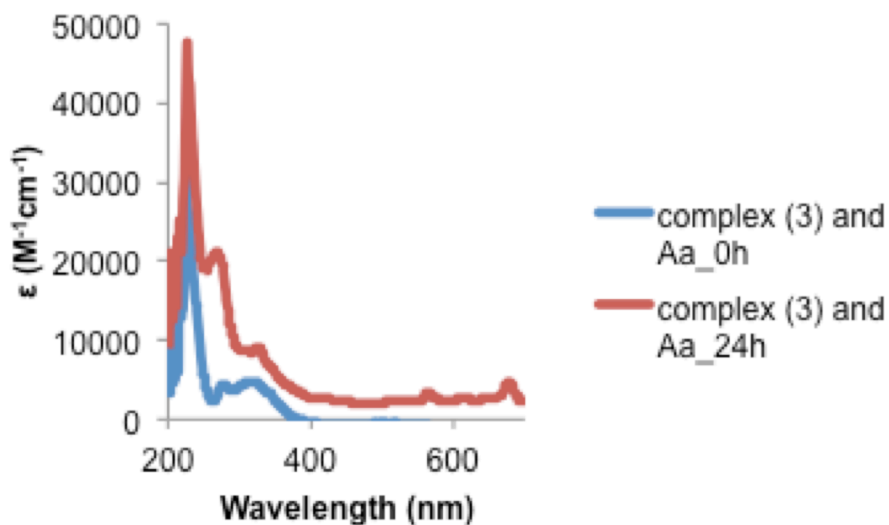


Figure 11. Ascorbic acid studies for ligand (1) at 20 °C and complex (3) at 37 °C

The stability profile of the ligand (2) and complex (4) in presence of GSH do not display any significant changes in their UV-vis spectrum over 24 hours (Figure 12.). At 20 °C, the λ_{\max} for the intraligand transitions for ligand (2) undergo a negligible decrease in intensity with increasing time. The absorption spectra for complex (4) at 20 °C and at 37 °C display a very similar profile.

There is a very small decrease in the intraligand bands transition intensity, and the LMCT band does not change significantly either. These results demonstrate the stability of the compounds and Au(III) in solution at different temperatures from undergoing reduction in presence of GSH (Figure 12.).

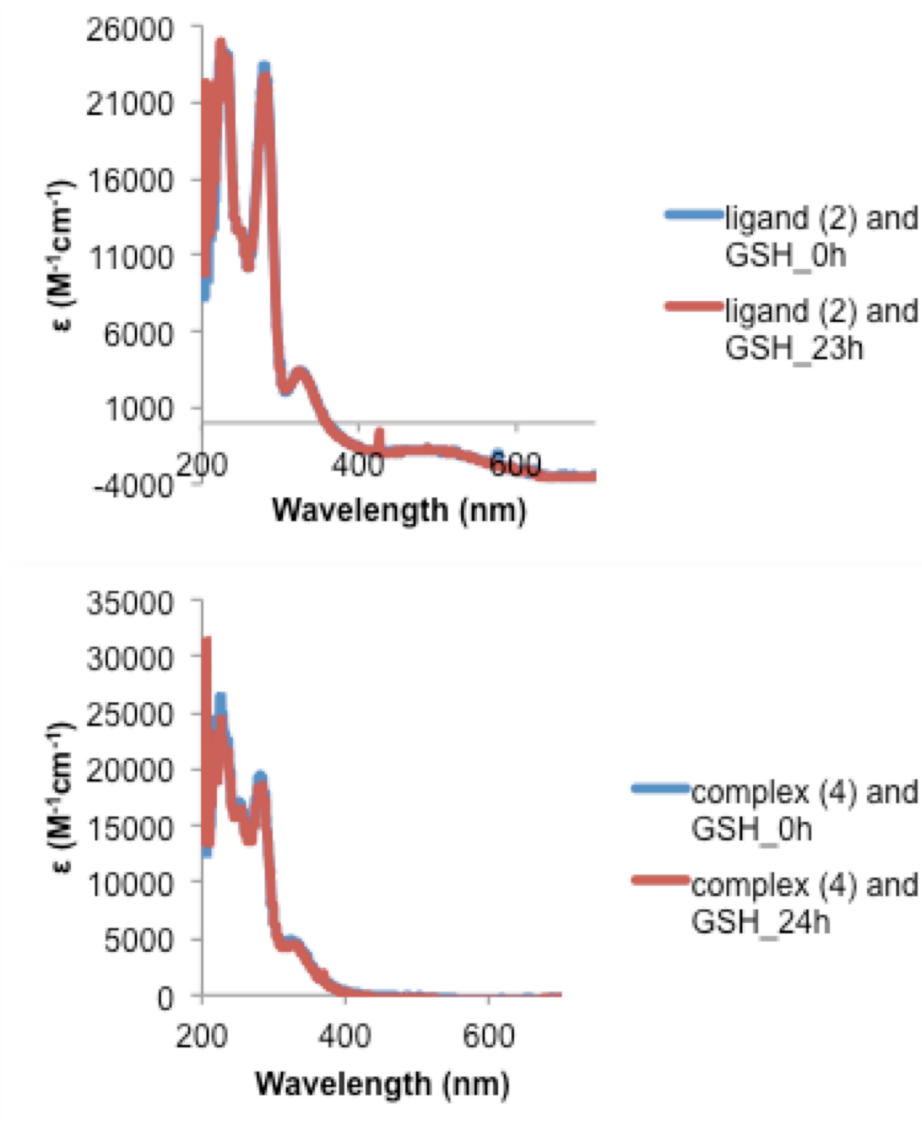


Figure 12. GSH studies for ligand (2) and complex (4) at 20 °C

Ligand (2) in presence of ascorbic acid displays a decrease in the intensity of its intraligand absorption bands at 233 and 281 nm with the peak at 329 nm not displaying any significant decrease over 24 hours (Figure 13.). For the complex (4) at 20 °C and at 37 °C display a similar profile to that of the complex (3). At 20 °C, the complex (4) shows a sharp decrease in the intensities of the intraligand transition bands and a small

change in the LMCT band. For the complex (4) at 37 °C two of the three intraligand transition bands (225, 290 nm) show a small increase, and the band at 269 nm displays a decrease in its intensity. The absorption peak corresponding to gold(I) at 450-520nm is not observed, suggesting the presence of Au in its +3 oxidation state in the solution.

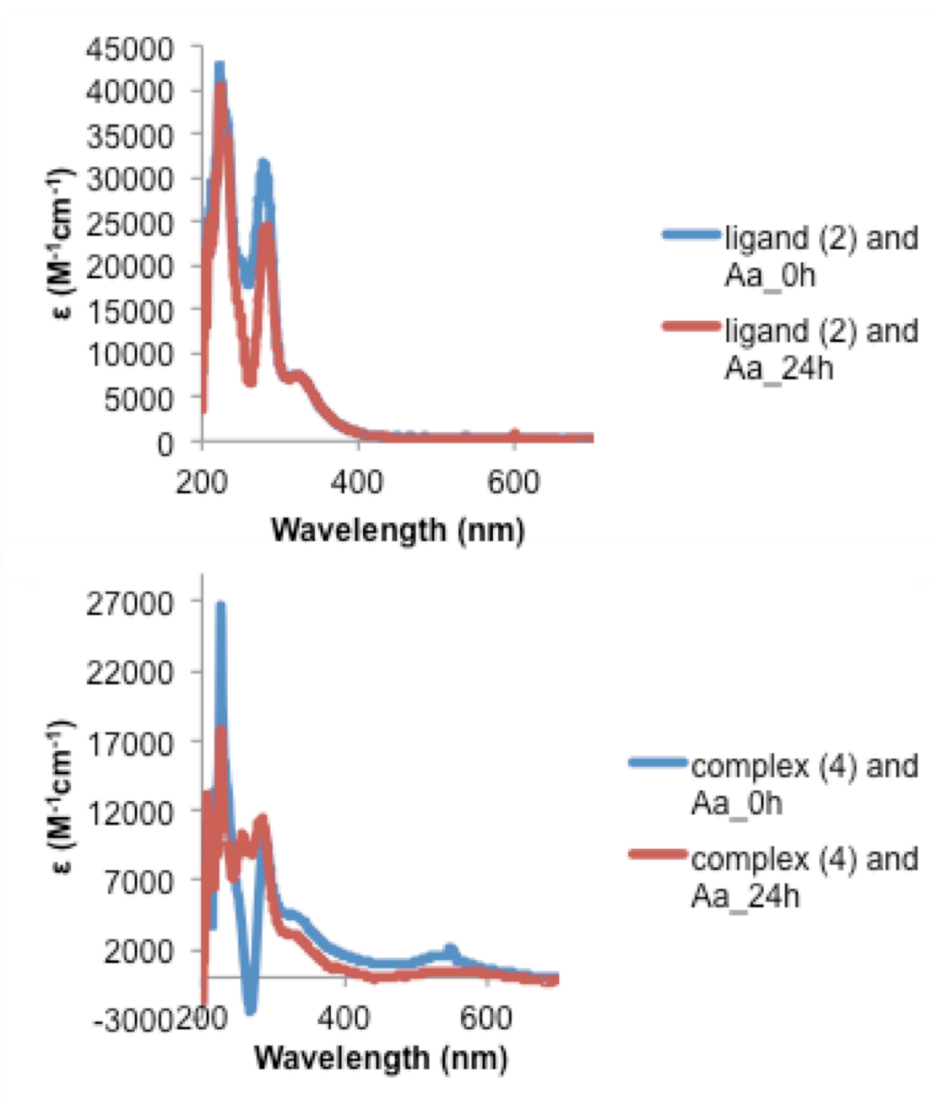


Figure 13. Ascorbic studies for ligand (2) at 20 °C and complex (4) at 37 °C

The LMCT band decreases by a negligible amount in intensity and in both the cases formation of colloidal gold was not observed (Figure 13.). The UV-visible profiles for the ligands and the complexes, at different temperatures indicate that the compounds are stable in the solution state. The Au(III) center is found to retain its oxidation state of +3 in most of the solutions and a comparison of the absorption spectra for the ligand and their complexes in buffered solutions and in presence of reducing agents, suggest towards presence of a charged or a cationic species in solution instead of the neutral complexes (3) and (4).

Calculation of logP²²

The logarithmic ratio of the concentration of a substance in two immiscible solvents is termed partition (Pt) coefficient, $\log P$. If the two-phase system used is octanol and water, then the ratio to calculate $\log P$ is given by $\text{Log } P = \log (\text{Pt})_{\text{octanol}} / (\text{Pt})_{\text{water}}$. This $\log P_{o/w}$ ratio determines if a given compound is primarily hydrophilic or lipophilic by nature. In general, a positive $\log P_{o/w}$ value implicates the compound is lipophilic and a negative $\log P_{o/w}$ value implies that the compound is hydrophilic.²² The $\log P_{o/w}$ value²³ for ligand (1) was found to be 1.56 +/- 0.73 and for ligand (2)²³ the value was found to be 0.61 +/- 0.72. These values indicate that the ligands have an appropriate profile for being hydrophilic to an extent of being tested *in vitro*, and are lipophilic to a suitable extent. The complexes prepared with these ligands can be predicted to have the ability to cross the lipid bilayer of cell membrane and also be stable in solution.

X-ray Crystallographic studies

X-ray quality crystals for the complexes (3) and (4) could not be obtained. The X-ray crystals for the monoprotonated ligand salt (1) and (2) were obtained by diffusion of diethyl ether into a solution of DMF and ethanol (ligand (1)), and diffusion of diethyl ether into a solution of DMF and methanol (ligand (2)). The molecular structures obtained over the hypothesis of presence of a cationic species instead of a neutral complex (3) and (4), as observed by their respective NMR, UV-visible and solubility test data. The molecular structure for cationic ligand (1) is shown in Figure 14. It shows the acidic proton residing at one of the nitrogen donors (N2B) on the phenanthroline ring.

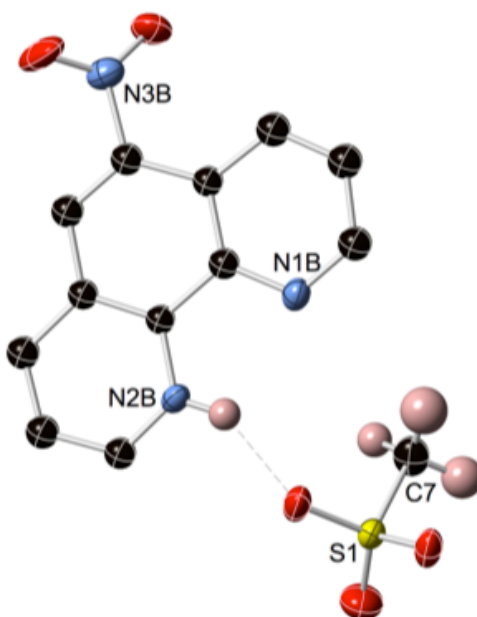


Figure 14. Molecular structure for [^{nitro}phenH]⁺[CH₃SO₃]⁻, protonated ligand (1)

The acidic proton is interacting with methyl sulfonate counterion through hydrogen bonding interactions. The protonated ligand (1) crystals were isolated from the

crystallization set up for complex (3). As the synthesis for complex (3) was carried out in DMSO, the gold(III) is possibly getting reduced to gold(I) and catalyzing the formation of the protonated species in the reduced environment. Methanesulfonic acid is a common impurity found in DMSO²⁴ and is evidenced to give rise to protonated species in solution and methane sulfonate anion.

The molecular structure for the monoprotonated ligand (2) is shown in Figure 15. One of the nitrogen (N2) on the phenanthroline ring is protonated. The Nitrogen of the substituted amine group is interacting with tetrafluoroborate counterion by hydrogen bonding. The tetrafluoroborate ion arises from the AgBF₄ reagent, being used in the synthesis step (Scheme 6.) for the preparation of complex (4). The crystal structure also reveals that the phenanthroline ring undergoes electrophilic halogenation on the backbone, where one of the hydrogen on the ring is substituted for a Cl⁻ group.

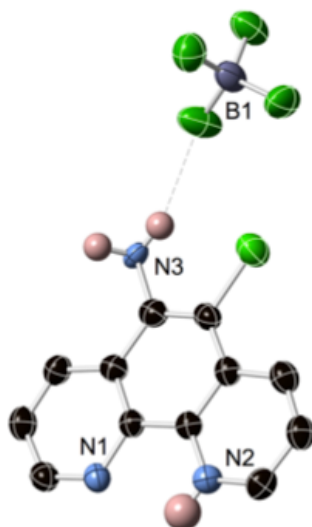


Figure 15. Molecular structure for [6-amino,5-chlorophenH]⁺[BF₄]⁻, protonated ligand (2)

The proposed mechanism of substitution is akin to the electrophilic aromatic substitution, where a lewis acid like, AlCl_3 , FeCl_3 or ZnCl_2 catalyze the reaction. In this reaction, the AuCl_3 from the reagent NaAuCl_4 (Scheme 6.) acts as a lewis acid catalyst, catalyzing the formation of an electrophilic complex that attacks the phenanthroline ring. The NH_2 substituted on the phenanthroline ring is a strong ortho and para activating group, directs the incoming electrophile to the ortho position, thereby bringing about chlorination of the phenanthroline ring.

Protonation of the ligands, while attempting the synthesis of gold(III) complexes stresses upon the need for a judicious choice of solvents and maintaining the overall basicity of the reaction system. To avoid the formation of protonated ligands, and promote metallation of the ligand, solvents with higher solvation energies were utilized. Using polar aprotic solvent combinations like ethanol/water, acetonitrile/water, that have been previously employed for the synthesis of gold(III) complexes with polypyridyl ligands²⁵. Water has high solvation energies and acetonitrile and methanol are relatively aprotic to protonate the ligand.²⁶ The basicity constant (K_b) for the ligands (Figure 16.) were calculated using a software²³ to ascertain the choice of solvents employed for synthesis, for it has been evidenced that the product of a reaction of gold(III) with N-bearing ligands depends on the acidity or basicity of the solution.²⁷

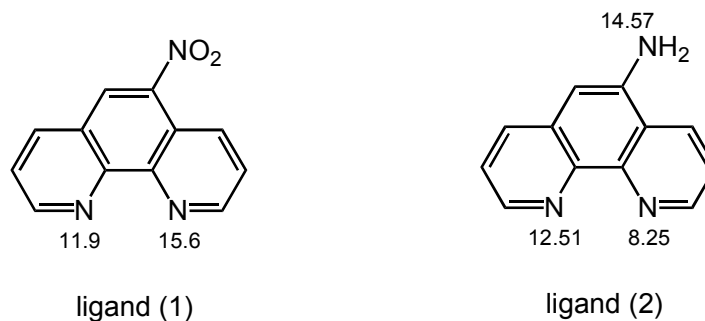


Figure 16. K_b values for ligand (1) and ligand (2)

Spectrophotometric and conductometric measurements carried out on AuX_3 ,phen complexes²⁶ ($X = Cl, Br$) demonstrate an equilibrium (Equation 1.) in solution between the reactants and the products when solvents such as nitrobenzene or acetone are used.²⁶ This equilibrium is not observed in aqueous solutions, resulting in product formation, due to the high solvation energy of water.²⁶

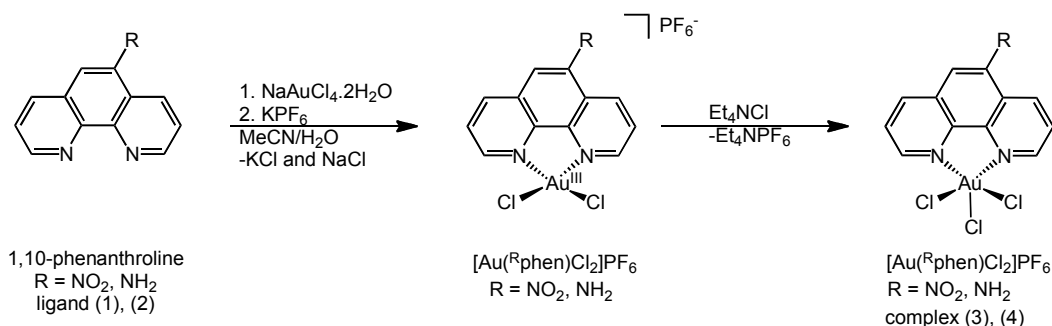


Equation 1. Reaction equilibrium between the reactants and products in non-aqueous solvents

Alternative synthetic approach

To promote the formation of gold(III) complex and prevent the protonation of the ligands a literature documented synthetic route was attempted.²⁵ The strategic route to prepare neutral gold(III) complexes, using this synthetic route, with ligand (1) and ligand (2) is to isolate the hexafluorophosphate salts of the complex with gold(III) and isolate

the neutral gold(III) complexes by precipitating them with a precipitating agent like tetraethylammonium chloride (Scheme 7.).



Scheme 7. Synthetic route for synthesis of complex (3) and (4), from the PF₆⁻ gold(III) salts

The PF₆⁻ complex with 1,10-phenanthroline ([Au(phen)Cl₂]PF₆⁻) has been successfully prepared and characterized in the MacBeth laboratory. A crystal structure for this complex has been successfully isolated. The reaction was carried out with ligand (1) and ligand (2). The prepared PF₆⁻ salts with ligand (1) and (2) displayed a poor solubility in organic solvents and were characterized by NMR, and IR spectroscopy. In both the cases, a crystal structure for the PF₆⁻ salt could not be isolated.

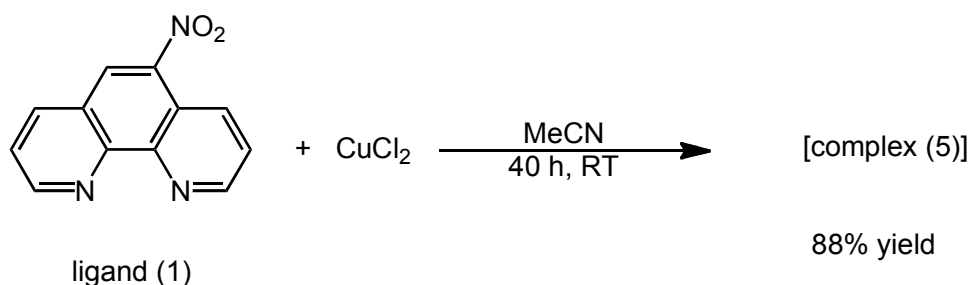
Synthesis of Cu(II) complexes

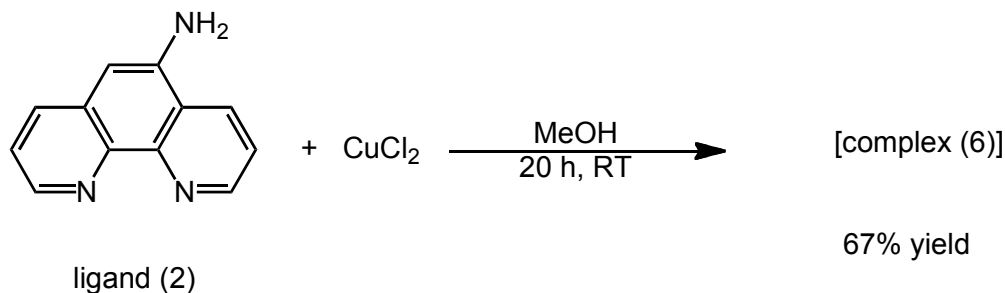
To understand the behavior of ligand (1) and (2) in solution state and explore the parameters required for a successful metallation with gold(III), copper(II) chloride complexes of the ligands were prepared. Copper belongs to the same row of transition metals as gold and chemistry of copper complexes is well documented in the literature. Cu(II) complexes have distinct characteristics in the UV-visible spectrum, which are

diagnostic of the nature of bonding, and type of complex present in the solution state.

A search of literature for CuCl_2 complexes prepared with ligands (1) and (2) revealed that CuCl_2 complexes of ligand (1) and (2) have not been documented as of yet. Literature examples of Cu(II) complexes with 1,10-phenanthroline as the ligand has been well documented.^{28,29} Examples of Cu(II) complexes with ligand (1) that are documented have been prepared with different equivalent ratios of ligands, as their CH_3CN complexes with BF_4^- as counter ion.³⁰ Cu(II) hydroxide complexes with diamine substituted 1,10-phenanthroline ligand³¹, coordination complexes with bipyridine and amine-substituted phenanthroline complexes³², are some of the examples of Cu(II) complexes with amine substituted phenanthroline found in the literature.

Synthesis of CuCl_2 complexes, complex (5) and complex (6), with ligands (1) and (2) was carried out (Scheme 8.) by adapting the literature synthesis procedures documented for similar complexes.^{28,30,33}





Scheme 8. Synthesis of complexes (5) and (6)

The complexes were prepared by reaction of an equimolar amount of CuCl₂ and the ligand (1) in MeCN, and ligand (2) in MeOH at room temperature. The complexes (5) and (6) were isolated as Turkish blue and yellow-green solids. The complexes prepared, have been characterized with UV-visible and IR and ESI-MS spectroscopy. The ¹H NMR data was difficult to evaluate and did not provide much information as the Cu(II) nucleus is paramagnetic in nature.

The UV-visible spectra for the ligands and complexes were recorded in methanol (Figure 17.). The ligand (1) shows absorption λ_{max} at 232, 267 and a broad shoulder at 322 – 353 nm, whereas complex (5) displays absorptions λ_{max} at 204, 239, 278 and a weak band centered at 323 nm. A redshift of the λ_{max} is observed for the complex (5) versus ligand (1). The $\pi \rightarrow \pi^*$ transitions for ligand (1) in the UV region are much stronger than that for the complex (5). The strong absorptions for ligand (1) can be attributed to the presence of the electron withdrawing nitro substituent on ligand (1).

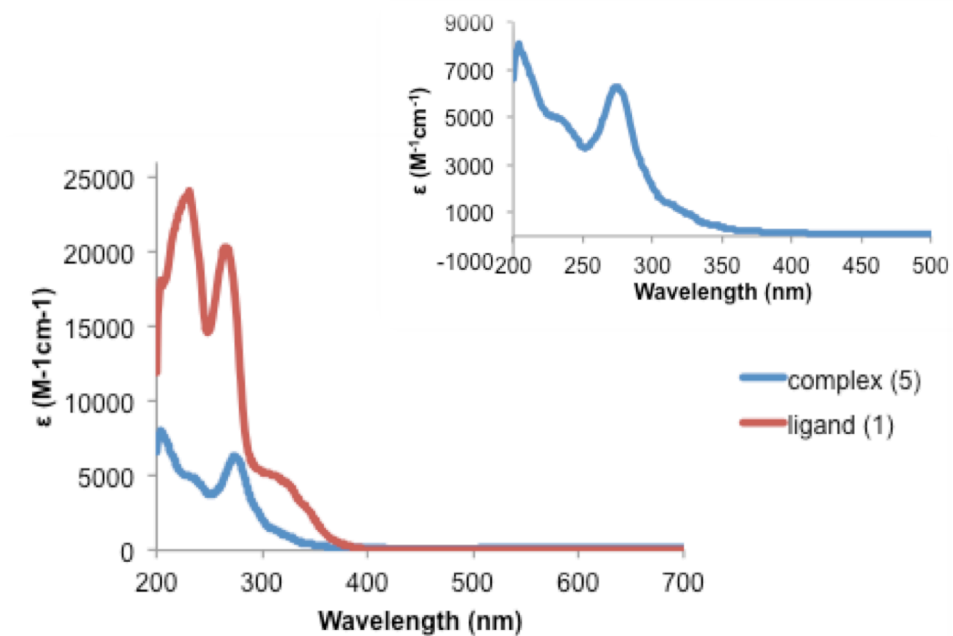


Figure 17. UV-visible spectra for complex (5) overlaid with spectra for ligand (1), room temperature, (1×10^{-4} M in Methanol); spectra for complex (5) provided as an inset for clarity

The ligand (2) shows absorption λ_{\max} at 222, 236, 283 and a shoulder at 344 nm, whereas complex (6) displays absorptions λ_{\max} at 213, 247, 267, 301 and a shoulder at 371 nm (Figure 18.). A different absorption spectrum with a redshifting of the absorption bands is observed for the complex (6) versus ligand (2). The $\pi \rightarrow \pi^*$ transitions for ligand (2) in the UV region are much stronger than that for the complex (5). The strong absorptions for ligand (1) can be attributed to the presence of the electron withdrawing nitro substituent on ligand (1).

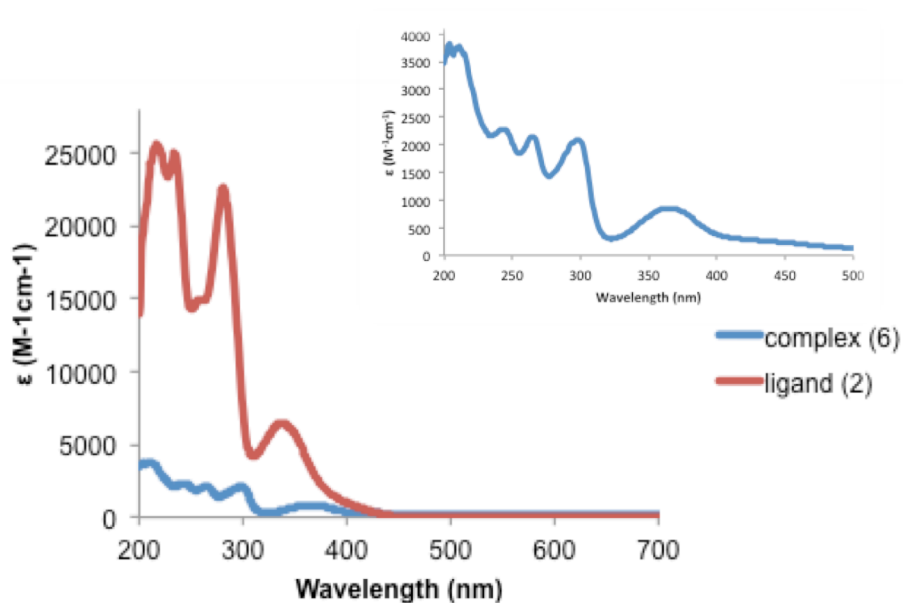


Figure 18. UV-visible spectra for complex (6) overlaid with spectra for ligand (2), room temperature, (1×10^{-4} M in Methanol); spectra for complex (6) provided as an inset for clarity

The ESI-MS spectra for the complexes (5) and (6) were collected. In the (MS) ESI spectrum, positive mode for complex (5) (Figure 19.) the base peak is a monomeric complex with a fragment of DMSO (the sample for ESI (MS) was prepared in DMSO). The base peak at $[m/z = 407.0 (100)]$ corresponds to $[(\text{nitrophen})\text{CuCl}_2(\text{CH}_3\text{S})]$, the peak at $[m/z = 275.1 (17)]$ corresponds to a fragment of ligand (1) along with a molecule of acetonitrile and 5 H^+ $[(\text{nitrophen})\text{CH}_8\text{CN}]$. In the negative mode, peak at $[m/z = 887.7 (93)]$ is probably constituted of a dimeric $[(\text{nitrophen})\text{CuCl}_2]_2$ with CuCl_2 , NO^- and 3H^+ fragments, the base peak at $[m/z = 527.8 (100)]$ corresponds to a monomeric

$[(^{\text{nitro}}\text{phen})\text{CuCl}_2)_2]$ with CuCl_2 , NO and 3H^+ , formed by the loss of dimeric form of the complex in solution.

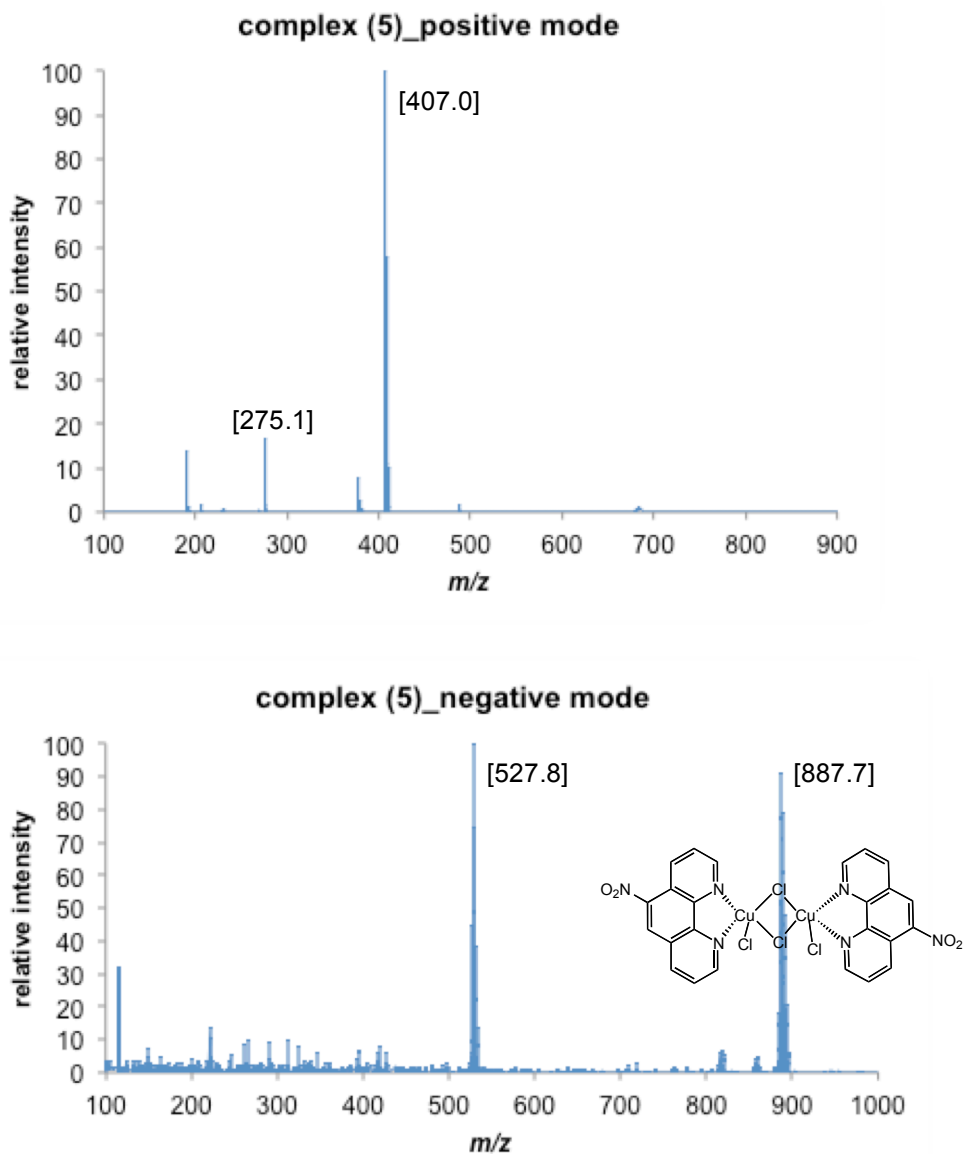


Figure 19. ESI-MS plots for complex (5), positive and negative mode

The MS (ESI) spectrum for the complex (6) (Figure 20.), in the negative mode shows the presence of a dimeric complex (6) along with a chloride anion $[(^{\text{amino}}\text{phen})\text{CuCl}_2)_2\text{Cl}]^-$ [m/z (%) = 694.9 (100)] and monomeric complex (6) with a molecule of methanol

$[(^{\text{amino}}\text{phen})\text{CuCl}_2(\text{CH}_3\text{OH}_2)]$ [m/z (%) = 362.9 (22)]. In the positive MS (ESI) mode shows a base peak with 100% relative intensity corresponding to a monomeric complex along with a molecule of water and methanol, $[(^{\text{amino}}\text{phen})\text{CuCl}_2(\text{CH}_3\text{OH})(\text{H}_2\text{O})]$ [m/z (%) = 377.0 (100)]. The data suggests presence of a dimeric complex in the solution state and partial conversion of the dimer into a monomeric species.

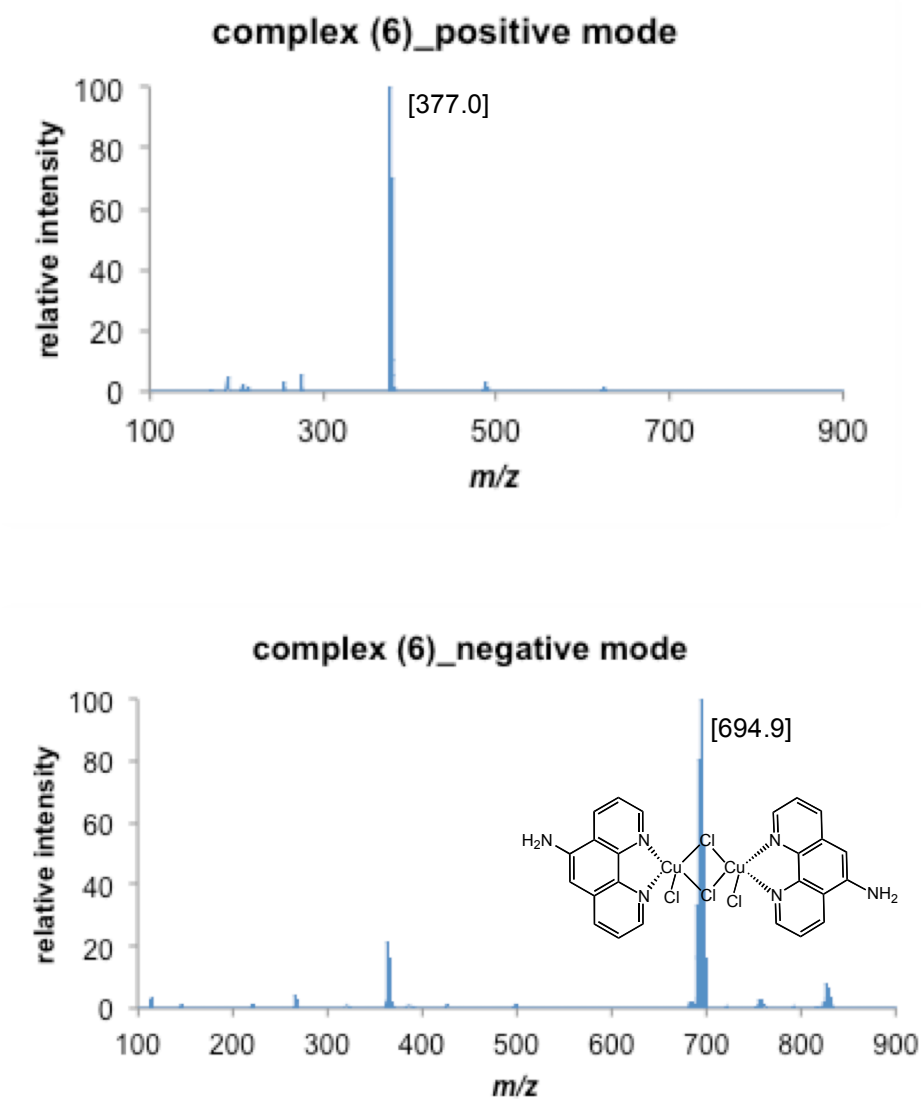


Figure 20. ESI-MS plots for complex (6), positive and negative mode

Synthesis of complexes (5) and (6) was attempted in a 1:1 stoichiometric ratio, to achieve the targeted molecules (Figure 21.). However the ESI-MS data shows the presence of a dimer in the solution state, with partial conversion into a monomeric species.

This observation of formation of a dimer in solution state while attempting to synthesize a monomer is not unprecedented and has been previously observed for Cu(II) complexes with 2,9-diaryl-1,10-phenanthroline complexes.³³ Moreover, when the UV-visible spectra for complexes (5) and (6) were compared with the UV-visible data for the dimeric CuCl₂ complex with the unsubstituted phenanthroline [(1,10-phenanthroline)₂CuCl₂], that has been previously reported³⁴, the spectra display a similar distribution of the absorption bands in the 200-400 nm region of the spectrum, as observed for complexes (5) and (6). The similarity of distribution of the absorption bands to the reported dimer, [(1,10-phenanthroline)₂CuCl₂] further supports the proposition of the presence of a dimeric complexes (5) and (6) in the solution state.

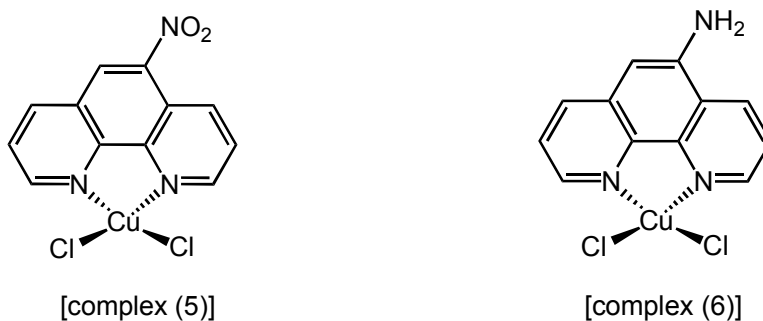


Figure 21. Targeted structures for complex (5) and (6)

The synthesis and characterization data acquired for the Cu(II) complexes prepared with ligands (1) and (2) gives an insight into the chemistry of the ligands and their preferential metallation patterns. Presence and formation of a dimeric species in solution state for complexes (5) and (6), as obtained in the ESI-MS results suggest a tendency to form dimeric complexes in solution. Formation of protonated species in presence of DMSO, while attempting the synthesis of complex (3) suggests reaction between DMSO and gold metals hindering the formation of neutral complexes. Success at synthesizing a PF_6^- salt complex with the 1,10-phenanthroline ligand and understanding the solvation properties of solvents provides information for designing synthetic routes that balance the overall basicity of the system by using aprotic solvents and isolating the complexes as gold(III) salts which can then be further worked up to isolate the neutral gold(III) complexes.

Conclusions

In conclusion, synthesis of two novel Au(III) complexes [(^{nitro}phenanthroline)AuCl₃] and [(^{amino}phenanthroline)AuCl₃] has been attempted and characterized by various spectroscopic techniques. Different synthetic protocols were experimented and employed for synthesizing pure complexes in high yields.

Initial characterization and spectroscopic data suggested the absence of a neutral complex and presence of a charged species. This hypothesis was later confirmed with crystal structures that demonstrated initial synthetic attempts leading to synthesis of protonated ligands versus neutral complexes. Based upon the data collected, importance of a judicious choice of solvents for synthesis and maintenance of the overall basicity of the reaction system has been realized to promote complex formation. The UV-visible spectroscopic data reveals that the ligands and the protonated ligands are stable in physiological buffered solutions. Absorption data did not show a loss of the +3 oxidation of gold in presence of reducing agents like GSH and ascorbic acid. Presence of reducing agents and increase in temperature were also observed to be unable to reduce the Au(III) center to form gold(I).

Synthesis of Cu(II) complexes with ligands (1) and (2) and studying their solution profile, reveals preference of dimer formation in solution albeit the attempted synthesis was in a 1:1 stoichiometric ratio. This data demonstrates the preference of complexes prepared with ligands (1) and (2) to dimerize in solution state, suggesting the synthesis of complexes with Au(III) in a 1:2 stoichiometric ratio to promote complex formation.

Experimental

General Considerations

The reagents used, AuCl_3 , $\text{NaAuCl}_4 \cdot 2\text{H}_2\text{O}$, AgBF_4 and 1,10-phenanthroline were purchased from commercial vendors and used as received unless otherwise noted. The solvents used were purchased without any further purification. Aside from eliminating direct exposure to sunlight, no specific handling measures were taken with the Au(III) complexes. The ^1H NMR spectra were recorded on Varian Mercury 300 and Inova 400 MHz spectrometers at ambient temperature; chemical shifts were referenced to residual solvent peaks. Infrared spectra were recorded as KBr pellets on a Varian Scimitar 800 Series FT-IR spectrophotometer. UV-visible absorption spectra were recorded on a Cary 50 spectrophotometer using 1.0 cm quartz cuvettes. Mass spectra were recorded in the Mass Spectrometry Center at Emory University on a JEOL JMS-SX102/SX102A/E mass spectrometer. X-ray diffraction studies were carried out in the X-ray Crystallography Laboratory at Emory University on a Bruker Smart 1000 CCD diffractometer.

Synthesis of 5-nitro-1,10-phenanthroline

The ligand was synthesized as per the literature procedure.¹⁸ 1,10-phenanthroline (2.00 g, 11.10 mmol) was dissolved in 12.0 mL concentrated H_2SO_4 . The system was refluxed at 160-170 °C and 6.0 mL concentrated HNO_3 was added to the refluxing solution drop-wise. This reaction mixture was refluxed under a nitrogen atmosphere for 3 h, and the solution was finally poured into ice water. The pH of this aqueous solution was normalized to pH = 3 by addition of 10 N NaOH. The product was a pale yellow precipitate that was filtered and washed with copious amounts of water. The product was

dried *in vacuo* overnight (74%, 1.84 g). ^1H NMR (δ , DMSO, 400 MHz): 7.93 (m, 2H), 8.76 (d, 1H, $J = 8$ Hz), 8.87 (d, 1H, $J = 8$ Hz), 9.01 (s, 1H), 9.25 (d, 2H, $J = 18$ Hz). FTIR (KBr, cm^{-1}): $\nu(\text{NO}_2)$ 1518, 1346. UV-vis (DMSO) λ_{max} , nm (ϵ , $\text{M}^{-1} \text{cm}^{-1}$): 239 (23100), 274 (29200), 324 (10000). UV-vis (MeOH) λ_{max} , nm (ϵ , $\text{M}^{-1} \text{cm}^{-1}$): 232 (23653), 267 (19844), 335 (3455).

Synthesis of 5-amino-1,10-phenanthroline

The ligand was prepared as per the literature procedure.¹⁸ 1,10-phenanthroline (1.00 g, 4.44 mmol) catalyst 5% Pd/C (0.26 g) was stirred in 20.0 mL absolute ethanol. The solution was heated to 70 °C under a nitrogen atmosphere. The reaction flask was covered with aluminum foil to protect the mixture from light. At 70 °C a solution of hydrazine monohydrate (1.00 g, 20.75 mmol) was prepared in 10.0 mL of absolute ethanol and was added dropwise over a period of 45 minutes to the reflux at 70 °C. The mixture was refluxed at 70 °C for 6 hours. After cooling, the solution was filtered over a bed of celite and the catalyst was washed with copious amounts of ethanol. The solution was evaporated on a rotavap and a yellow solid was left behind. The solid was washed with chloroform and a green impurity was filtered off to leave behind a yellow solid. The yellow product was dried *in vacuo* overnight (92%, 0.80 g). ^1H NMR (δ , DMSO, 300 MHz): 6.14 (s, 2H, NH_2), 6.85 (s, 1H), 7.51 (m, 1H), 7.73 (m, 1H), 8.67 (m, 2H), 8.04 (d, 2H, $J = 8$ Hz), 9.05 (d, 1H, $J = 4$ Hz) FTIR (KBr, cm^{-1}): $\nu(\text{NH}_2)$ 3474, 3382. UV-vis (DMSO) λ_{max} , nm (ϵ , $\text{M}^{-1} \text{cm}^{-1}$): 233 (17400), 284 (22300), 329 (4700). UV-vis (MeOH) λ_{max} , nm (ϵ , $\text{M}^{-1} \text{cm}^{-1}$): 222 (24922), 236 (24607), 283 (22198), 344 (shoulder, 6208).

Synthesis of [^{nitro}phenH]⁺[CH₃SO₃]:

The ligand, 5-nitro-1,10-phenanthroline (0.048 g, 0.213 mmol) and AuCl₃ (0.067 g, 0.221 mmol) were dissolved in 8 – 10.0 mL DMSO. This reaction mixture was refluxed at 65 °C under a nitrogen atmosphere for 24 h, and the solution remained a clear yellow throughout. The solvent was evaporated over the schlenk line and a pale yellow solid was isolated. The solid was washed with diethyl ether (x 3) to give a yellow-orange colored product. The product was dried *in vacuo* overnight (98%, 0.11 g). ¹H NMR (δ, DMSO, 300 MHz): 8.11 (m, 2H), 9.00 (d, 1H, *J* = 8 Hz), 9.06 (d, 1H, *J* = 9 Hz), 9.18 (s, 1H), 9.31 (d, 1H, *J* = 4 Hz), 9.36 (d, 1H, *J* = 5 Hz). ¹³C NMR (δ, DMSO, 100 MHz): 100.17, 121.72, 126.35, 126.45, 125.56, 126.83, 136.47, 143.98, 144.17, 149.85, 150.45. HRMS(ESI): C₁₂H₇N₃O₂ *m/z*. Calcd. 528.38, Found 226.1 [M-AuCl₃]. FTIR (KBr, cm⁻¹): ν(NO₂) 1524, 1351. UV-vis (DMSO) λ_{max}, nm (ε, M⁻¹ cm⁻¹): 242 (31100), 280 (25000), 314-334 (broad shoulder).

Synthesis of [^{6-amino,5-chloro}phenH]⁺[BF₄]:

The ligand, 5-amino-1,10-phenanthroline (0.15 g, 0.768 mmol) was dissolved in 40.0 mL of methanol. NaAuCl₄•2H₂O (0.31 g, 0.769 mmol) and AgBF₄ (0.15 g, 0.77 mmol) were dissolved in 3 - 4.0 mL of methanol individually and were added to the ligand solution. The mixture was refluxed at 65 °C overnight upon which a dark orange solution was formed. The reaction was allowed to cool to room temperature and AgCl, the precipitate was filtered over a celite pad. The solvent was removed over the rotavap and product was isolated as a dark red-orange solid. The product was dried *in vacuo* overnight (60%, 0.23 g). ¹H NMR (δ, DMSO, 400 MHz): 7.18 (brs, 2H), 8.13 (m, 2H), 8.84 (d, 1H, *J* = 8 Hz),

8.90 (d, 1H, $J = 5$ Hz), 9.18 (d, 1H, $J = 9$ Hz), 9.26 (d, 1H, $J = 4$ Hz). ^{13}C NMR (δ , DMSO, 100 MHz): 102.52, 122.18, 125.32, 125.95, 129.17, 134.66, 135.84, 138.09, 140.74, 140.95, 149.23. HRMS(ESI): $\text{C}_{12}\text{H}_9\text{N}_3$ m/z Calcd. 498.547, Found 463.173 [M-Cl] $^+$. FTIR (KBr, cm^{-1}): $\nu(\text{NH}_2)$ 3474, 3382. UV-vis (DMSO) λ_{max} , nm (ϵ , $\text{M}^{-1} \text{cm}^{-1}$): 227 (35300), 267 (19100), 290 (13500), 355-372 (broad shoulder).

Synthesis of $[\text{Au}(\text{nitrophen})\text{Cl}_2]\text{PF}_6^-$

The ligand, 5-nitro-1,10-phenanthroline (0.098 g, 0.435 mmol) was dissolved in ca. 6.0 mL MeCN and added to a solution of $\text{NaAuCl}_4 \cdot 2\text{H}_2\text{O}$ (0.173 g, 0.435 mmol) dissolved in ca. 6.0 mL D.I H_2O to give a yellow suspension. Solid KPF_6 (0.41 g, 2.238 mmol) was added as to the stirring suspension. The reaction mixture was set to reflux at 96°C under a nitrogen atmosphere for 22 h, and the system went from yellow to an orange-yellow suspension. The suspension was filtered and yellow product was collected that was washed with copious amounts of D.I H_2O to dissolve residues of KCl and NaCl present in the product. The product was dried overnight (86%, 0.26 g). ^1H NMR (δ , CD_6O , 400 MHz): 8.80 (m, 2H), 9.72 (d, 1H, $J = 17$ Hz), 9.91 (m, 2H), 10.10 (s, 2H). UV-vis (DMSO) λ_{max} , nm (ϵ , $\text{M}^{-1} \text{cm}^{-1}$): 227 (34008), 283 (5392).

Synthesis of $[\text{Au}(\text{amino phen})\text{Cl}_2]\text{PF}_6^-$

The ligand, 5-amino-1,10-phenanthroline (0.102 g, 0.523 mmol) was dissolved in ca. 10.0 mL MeCN and added to a solution of $\text{NaAuCl}_4 \cdot 2\text{H}_2\text{O}$ (0.209 g, 0.525 mmol) dissolved in ca. 5.0 mL D.I H_2O to give an intense red-orange suspension. Solid KPF_6 (0.48 g, 2.627 mmol) was added as to the stirring suspension. The reaction mixture was

set to reflux at 98° C under a nitrogen atmosphere for 22 h, and the system remains an orange-red suspension. The suspension was filtered; red-orange product was collected that was washed with copious amounts of D.I H₂O to dissolve residues of KCl and NaCl present in the product. The product was dried for two days (79%, 0.25 g). ¹H NMR (δ, DMSO, 300 MHz): 7.73 (s, 2H), 8.26 (m, 2H), 8.42 (m, 1H), 8.98 (d, 1H, *J* = 9 Hz), 9.32 (d, 1H, *J* = 6 Hz), 9.59 (d, 1H, *J* = 8 Hz), 9.69 (d, 2H, *J* = 6 Hz). UV-vis (DMSO) λ_{max}, nm (ε, M⁻¹ cm⁻¹): 229 (11943), 268 (7764), 314 (6388), 380 (2111), 475 (broad shoulder, 477).

Synthesis [Cu(^{nitro}phen)Cl₂]:

The ligand, 5-nitro-1,10-phenanthroline (0.107 g, 0.475 mmol) was dissolved in ca. 10.0mL MeCN and added to a solution of CuCl₂ (0.064 g, 0.476 mmol) dissolved in ca. 12.0 mL MeCN to give a Turkish blue suspension. The reaction mixture was set to stir at room temperature for 40 h, and the system remained a Turkish blue suspension throughout. The suspension was filtered and the Turkish blue product was collected. The product was dried for two days (88%, 0.15 g). HRMS(ESI): C₁₂H₇N₃O₂CuCl₂ *m/z* Calcd. 359.65, Found 407.0 [(^{nitro}phen)CuCl₂(CH₃S)]⁺, FTIR (KBr, cm⁻¹): 3047, 1626, 1608, 1584, 1536, ν(NO₂) 1514, 1445, 1421, ν(NO₂) 1331, 1205, 1152, 1118, 838, 817, 754, 734, 721, 649. UV-vis (MeOH) λ_{max}, nm (ε, M⁻¹ cm⁻¹): 204 (8085), 239 (4624), 278 (6142), 323 (999).

Synthesis [Cu(^{amino}phen)Cl₂]:

The ligand, 5-amino-1,10-phenanthroline (0.097 g, 0.497 mmol) was dissolved in ca.

10.0 mL MeOH and added to a solution of CuCl₂ (0.067 g, 0.498 mmol) dissolved in ca. 9.0 mL MeOH to give an intense red-orange suspension forms that changes to an intense green-yellow within the first 5 minutes of mixing the reagents and stirring the mixture. The reaction mixture was set to stir at room temperature for 20 h, and the system remained an intense green-yellow suspension throughout. The suspension was filtered and the green-yellow product was collected. The product was dried overnight (67%, 0.11 g). HRMS(ESI): C₁₂H₉N₃CuCl₂ *m/z* Calcd. 329.67, Found 694.9 [(^{amino}phen)CuCl₃]⁻, FTIR (KBr, cm⁻¹): ν(NH₂) 3430 and 3334, 3222, 3064, 1629, 1601, 1585, 1536, 1519, 1493, 1466, 1434, 1347, 1319, 1282, 1227, 1163, 1139, 1122, 1078, 908, 865, 799, 723, 646, 666, 430. UV-vis (MeOH) λ_{max}, nm (ε, M⁻¹ cm⁻¹): 213 (3702), 247 (2218), 267 (2107), 301 (2028), 371 (shoulder, 830).

Solution Studies

A 8 x 10⁻³ M stock solution of 5-nitro-1,10-phenanthroline and 1 x 10⁻² M stock solution of 5-amino-1,10-phenanthroline ligands was prepared by dissolving a 0.010 g sample in 5.0 mL of DMSO. A 3.0 μL aliquot of the ligand stock solutions was diluted to a final volume of 3.0 mL in phosphate buffer (pH = 7.4), yielding a ligand concentration of 1 x 10⁻⁵ M.

A 4 x 10⁻³ M stock solution of the gold complexes was prepared in 5.00 mL of DMSO. A 7.9 μL aliquot of the complex (3) stock solution and a 7.5 μL aliquot of the complex (4) stock solution was diluted to a final volume of 3.00 mL in phosphate buffer, yielding a gold concentration of 1 x 10⁻⁵ M. UV-visible spectra for ligands (1), (2) and complexes (3), (4) was collected over a period of 24 hours at 20 °C.

Solution studies in presence of biological reductants

The ligands (1), (2) and complexes (3), (4) stock solutions prepared for solution studies were used. A 6×10^{-3} M ascorbic acid stock solution and a 3×10^{-3} M glutathione stock solution was prepared by dissolving ascorbic acid or glutathione in distilled water. A 7.9 μ L aliquot of the complex (3) stock solution and a 7.5 μ L aliquot of the complex (4) stock solution was added to a 5.0 μ L of the ascorbic acid/ 9.0 μ L of glutathione and diluted in 0.1 M phosphate buffer with pH = 7.4 to a final volume of 3.0 mL. The final gold concentration of solution was 1×10^{-5} M. The solutions were prepared in a 1:1 ratio of the ligand or complex to ascorbic acid or glutathione. The UV-visible spectra of ligands (1), (2) and complexes (3), (4) was collected every hour over a time period of 24 hours at 20 °C. These stability experiments were also carried out for complexes (3), (4) at 37 °C.

UV-visible spectroscopic studies on Cu(II) complexes:

A 8×10^{-3} M stock solution of ligand (1) and 1×10^{-2} M stock solution of ligand (2) was prepared by dissolving a 0.010 g sample in 5.0 mL of MeOH. A 33.8 μ L aliquot of ligand (1) and a 29.3 μ L aliquot of ligand (2) stock solutions was diluted to a final volume of 3.0 mL in MeOH, yielding final ligand concentrations of 1×10^{-4} M. UV-visible spectra for ligands (1) and (2) were collected at 20 °C.

A 5.5×10^{-3} M stock solution of the complex (5) was prepared in 5.00 mL of MeOH. A 53.9 μ L aliquot of complex (5) stock solution was diluted to a final volume of 3.00 mL in MeOH, yielding a final concentration of 1×10^{-4} M. UV-visible spectra for complex (5) was collected at 20 °C.

A 6.1×10^{-3} M stock solution of the complex (6) was prepared in 5.00 mL of MeOH. A 49.4 μ L aliquot of complex (6) stock solution was diluted to a final volume of 3.00 mL in MeOH, yielding a final concentration of 1×10^{-4} M. UV-visible spectra for complex (6) was collected at 20 °C.

X-ray Crystallographic Data:

Table 1. Crystal refinement data for [nitrophenH]⁺[CH₃SO₃]⁻

Empirical formula	C ₂₆ H ₂₂ N ₆ O ₁₀ S ₂
Formula weight	642.62
Temperature/K	173
Crystal system	orthorhombic
Space group	P2 ₁ 2 ₁ 2 ₁
a/Å	8.1777(19)
b/Å	15.246(3)
c/Å	21.327(5)
α /°	90.00
β /°	90.00
γ /°	90.00
Volume/Å ³	2658.9(11)
Z	4
ρ_{calc} mg/mm ³	1.605
m/mm ⁻¹	0.274

F(000)	1328.0
Crystal size/mm ³	0.477 × 0.408 × 0.188
2 Θ range for data collection	3.28 to 51.36°
Index ranges	-9 ≤ h ≤ 9, -18 ≤ k ≤ 12, -23 ≤ l ≤ 26
Reflections collected	15627
Independent reflections	5044[R(int) = 0.0671]
Data/restraints/parameters	5044/15/302
Goodness-of-fit on F ²	1.061
Final R indexes [I ≥ 2σ(I)]	R ₁ = 0.0598, wR ₂ = 0.1377
Final R indexes [all data]	R ₁ = 0.0845, wR ₂ = 0.1520
Largest diff. peak/hole / e Å ⁻³	0.75/-0.31

Table 2. Crystal refinement data for [6-amino,5-chloro phenH]⁺[BF₄]⁻

Empirical formula	C ₁₅ H ₁₆ BClF ₄ N ₄ O
Formula weight	390.58
Temperature/K	446.35
Crystal system	monoclinic
Space group	C2/c
a/Å	19.918(4)
b/Å	12.912(2)
c/Å	13.305(3)
α/°	90.00

$\beta/^\circ$	100.093(3)
$\gamma/^\circ$	90.00
Volume/ \AA^3	3368.8(11)
Z	8
$\rho_{\text{calc}}/\text{mg}/\text{mm}^3$	1.540
μ/mm^{-1}	0.281
F(000)	1600
Crystal size/ mm^3	$0.572 \times 0.113 \times 0.094$
2 Θ range for data collection	4.66 to 56.68 $^\circ$
Index ranges	$-22 \leq h \leq 26, -17 \leq k \leq 16, -17 \leq l \leq 17$
Reflections collected	12283
Independent reflections	4180[R(int) = 0.0553]
Data/restraints/parameters	4180/0/239
Goodness-of-fit on F^2	1.054
Final R indexes [$I \geq 2\sigma(I)$]	$R_1 = 0.0735, wR_2 = 0.1980$
Final R indexes [all data]	$R_1 = 0.1460, wR_2 = 0.2330$
Largest diff. peak/hole / $e \text{\AA}^{-3}$	0.602/-0.606

References

1. Gabbiani, C. C., A.; Messori, L., Gold(III) compounds as anticancer drugs. *Gold Bull* **2007**, *40* (1), 73-81.
2. Berners-Price, S. J., Gold-Based Therapeutic Agents: A New Perspective. In *Bioinorganic Medicinal Chemistry*, Alessio, E., Ed. Wiley-VCH Verlag GmbH & Co. KGaA, Weinheim: 2011; pp 197-222.
3. Sanghvi, C. D. Synthesis, characterization and in vitro biological testing of gold(III) polypyridyl coordination compounds: Cytotoxicity of neutral, distorted square pyramidal complexes. Emory University, Atlanta, 2011.
4. Jemal, A.; Bray, F.; Center, M. M.; Ferlay, J.; Ward, E.; Forman, D., Global cancer statistics. *CA: a cancer journal for clinicians* **2011**, *61* (2), 69-90.
5. Kelland, L. R., Cisplatin-based Anticancer Agents. In *Uses of Inorganic Chemistry in Medicine*, Farrell, N. P., Ed. The Royal Society of Chemistry: 1999; pp 109-123.
6. III, C. F. S., Gold complexes with anti-arthritic, anti-tumour and anti-HIV activity. In *Uses of Inorganic Chemistry in Medicine*, Farrell, N. P., Ed. The Royal Society of Chemistry: 1999.
7. Milacic, V.; Dou, Q. P., The tumor proteasome as a novel target for gold(III) complexes: implications for breast cancer therapy. *Coordination chemistry reviews* **2009**, *253* (11-12), 1649-1660.
8. Hudson, Z. D.; Sanghvi, C. D.; Rhine, M. A.; Ng, J. J.; Bunge, S. D.; Hardcastle, K. I.; Saadein, M. R.; MacBeth, C. E.; Eichler, J. F., Synthesis and characterization of

gold(III) complexes possessing 2,9-dialkylphenanthroline ligands: to bind or not to bind? *Dalton transactions* **2009**, (36), 7473-80.

9. (a) Bruijninx, P. C. A.; Sadler, P. J., New trends for metal complexes with anticancer activity. *Current Opinion in Chemical Biology* **2008**, *12* (2), 197-206; (b) Casini, A.; Cinellu, M. A.; Minghetti, G.; Gabbiani, C.; Coronello, M.; Mini, E.; Messori, L., Structural and Solution Chemistry, Antiproliferative Effects, and DNA and Protein Binding Properties of a Series of Dinuclear Gold(III) Compounds with Bipyridyl Ligands. *Journal of Medicinal Chemistry* **2006**, *49* (18), 5524-5531.
10. Bindoli, A.; Rigobello, M. P.; Scutari, G.; Gabbiani, C.; Casini, A.; Messori, L., Thioredoxin reductase: A target for gold compounds acting as potential anticancer drugs. *Coordination Chemistry Reviews* **2009**, *253* (11-12), 1692-1707.
11. Balendiran, G. K.; Dabur, R.; Fraser, D., The role of glutathione in cancer. *Cell Biochemistry and Function* **2004**, *22* (6), 343-352.
12. Bertini, I., *Biological inorganic chemistry : structure and reactivity*. University Science Books: Sausalito, CA, 2007.
13. Wang, D.; Lippard, S. J., Cellular processing of platinum anticancer drugs. *Nature Reviews Drug Discovery* **2005**, *4* (4), 307-320.
14. Zhong, L.; Arner, E. S.; Holmgren, A., Structure and mechanism of mammalian thioredoxin reductase: the active site is a redox-active selenolthiol/selenenylsulfide formed from the conserved cysteine-selenocysteine sequence. *Proceedings of the National Academy of Sciences of the United States of America* **2000**, *97* (11), 5854-9.
15. Casini, A.; Hartinger, C.; Gabbiani, C.; Mini, E.; Dyson, P. J.; Keppler, B. K.; Messori, L., Gold(III) compounds as anticancer agents: relevance of gold-protein

interactions for their mechanism of action. *Journal of inorganic biochemistry* **2008**, *102* (3), 564-75.

16. (a) Zhao, G. S., H.; Lin, H.; Zhu, S.; Su, X.; Chen, Y. , Palladium(II) complexes with N,N'-Dialkyl-1,10-phenanthroline-2,9-dimethanamine: synthesis, characterization and cytotoxic activity. *Inorganic Biochemistry* **1998**, *72*; (b) Aguirre, J. D.; Angeles-Boza, A. M.; Chouai, A.; Turro, C.; Pellois, J. P.; Dunbar, K. R., Anticancer activity of heteroleptic diimine complexes of dirhodium: a study of intercalating properties, hydrophobicity and in cellulo activity. *Dalton transactions* **2009**, (48), 10806-12; (c) Heffeter, P.; Jakupec, M.; Korner, W.; Wild, S.; Vonkeyserlingk, N.; Elbling, L.; Zorbas, H.; Korynevskaya, A.; Knasmüller, S.; Sutterluty, H., Anticancer activity of the lanthanum compound [tris(1,10-phenanthroline)lanthanum(III)]trithiocyanate (KP772; FFC24). *Biochemical Pharmacology* **2006**, *71* (4), 426-440.
17. Hudson, Z. D. Synthesis, Characterization and Biological Data for Potential Anticancer Gold(III) Complexes. Emory University, Atlanta, 2010.
18. Binnemans, K.; Lenaerts, P.; Driesen, K.; Grolller-Walrand, C., A luminescent tris(2-thenoyltrifluoroacetato)europium(III) complex covalently linked to a 1,10-phenanthroline-functionalised sol-gel glass. *Journal of Materials Chemistry* **2004**, *14* (2), 191.
19. Chiara Gabbiani, A. G., Luigi Messori, Dinuclear Gold(III) Complexes as Potential Anticancer Agents: Structure, Reactivity and Biological Profile of a Series of Gold(III) Oxo-Bridged Derivatives. *The Open Crystallography Journal* **2010**, *3*, 29-40.

20. Casini, A.; Diawara, M. C.; Scopelliti, R.; Zakeeruddin, S. M.; Gratzel, M.; Dyson, P. J., Synthesis, characterisation and biological properties of gold(III) compounds with modified bipyridine and bipyridylamine ligands. *Dalton transactions* **2010**, 39 (9), 2239-45.
21. IKEIGHLEY, H. B. A. G., OXIDATION-REDUCTION POTENTIAL OF ASCORBIC ACID (VITAMIN C). In *PHYSIOLOGY: BORSOOK AND KEIGHLEY*, 1993; Vol. 19.
22. Roy, S.; Westmaas, J. A.; Hagen, K. D.; van Wezel, G. P.; Reedijk, J., Platinum(II) compounds with chelating ligands based on pyridine and pyrimidine: DNA and protein binding studies. *Journal of inorganic biochemistry* **2009**, 103 (9), 1288-97.
23. <http://www.organic-chemistry.org/prog/peol/>.
24. Szabó, P. T.; Kele, Z., Electrospray mass spectrometry of hydrophobic compounds using dimethyl sulfoxide and dimethylformamide as solvents. *Rapid Communications in Mass Spectrometry* **2001**, 15 (24), 2415-2419.
25. Palanichamy, K.; Ontko, A. C., Synthesis, characterization, and aqueous chemistry of cytotoxic Au(III) polypyridyl complexes. *Inorganica Chimica Acta* **2006**, 359 (1), 44-52.
26. Harris, C. M., 136. Nitrogenous chelate complexes of transition metals. Part I. The constitution and properties of the 1 : 10-phenanthroline complexes of tervalent gold. *Journal of the Chemical Society (Resumed)* **1959**, 682.
27. <Au(III) complex with bidentate lig (nitro-phenan lig)_Bailar_JACS_1951.pdf>.

28. Detoni, C.; Carvalho, N. d. M. F.; Aranda, D. A. G.; Louis, B.; Antunes, O. A. C., Cyclohexane and toluene oxidation catalyzed by 1,10-phenantroline Cu(II) complexes. *Applied Catalysis A: General* **2009**, *365* (2), 281-286.
29. Canhota, F. P.; Salomé, G. C.; Carvalho, N. d. M. F.; Antunes, O. A. C., Cyclohexane oxidation catalyzed by 2,2'-bipyridil Cu(II) complexes. *Catalysis Communications* **2008**, *9* (1), 182-185.
30. Bush, P. M.; Whitehead, J. P.; Pink, C. C.; Gramm, E. C.; Eglin, J. L.; Watton, S. P.; Pence, L. E., Electronic and Structural Variation among Copper(II) Complexes with Substituted Phenanthrolines. *Inorganic Chemistry* **2001**, *40* (8), 1871-1877.
31. Wall, M.; Linkletter, B.; Williams, D.; Hynes, R. C.; Chin, J., Rapid Hydrolysis of 2,3-cAMP with a Cu(II) Complex: Effect of Intramolecular Hydrogen Bonding on the Basicity and Reactivity of a Metal-Bound Hydroxide. *Journal of the American Chemical Society* **1999**, *121* (19), 4710-4711.
32. Marino, N.; Ikotun, O. F.; Julve, M.; Lloret, F.; Cano, J.; Doyle, R. P., Pyrophosphate-Mediated Magnetic Interactions in Cu(II) Coordination Complexes. *Inorganic Chemistry* **2010**, *50* (1), 378-389.
33. Yang, P.; Yang, X.-J.; Wu, B., Synthesis, Structure, and Spectroscopic and Electrochemical Properties of Copper(II/I) Complexes with Symmetrical and Unsymmetrical 2,9-Diaryl-1,10-phenanthroline Ligands. *European Journal of Inorganic Chemistry* **2009**, *2009* (20), 2951-2958.
34. Ying Li Mingzhu Wu Wei Liu Zhongzhou Yi Jucheng, Z., Selective Oxidation of Cyclohexane to Cyclohexanone Catalyzed by Phenanthroline-CuCl₂ Complex. *Catalysis Letters* **2008**, *123* (1/2), 123.